Acta Astronautica 212 (2023) 284–306

Contents lists available at ScienceDirect

Acta Astronautica

journal homepage: www.elsevier.com/locate/actaastro

Review Article

Review of alternative propellants in Hall thrusters

Vlad-George Tirila [a,*,1], Alain Demairé [b,2], Charles N. Ryan [a,3]

[a] University of Southampton, Astronautics Group, Faculty of Engineering and Physical Sciences, SO17 1BJ, Southampton, United Kingdom
[b] OHB Sweden AB, P.O Box 1269, SE-164 29, Kista, Sweden

ARTICLE INFO

MSC:
00-01
99-00

Keywords:
Hall thruster
Electric propulsion
Propellants
Review
Thruster database
Performance analysis
Molecular propellants
Condensable propellants

ABSTRACT

Hall thrusters, the most common type of electric propulsion system, typically use xenon as the propellant, given its inertness, its ability to be stored at a high density under pressure, and good thrust to power ratio coupled with a high specific impulse compared to chemical propulsion. However, the number of satellites utilizing electric propulsion units and particularly Hall thrusters is dramatically increasing, resulting in a strain on the availability of xenon propellant in the context of a volatile noble gas market. This phenomenon is seen with the dawn of large satellite constellations and the accelerated launch rate of satellite units, the majority of which now use a Hall thruster as their primary propulsion system. Alternatives to xenon are available in the form of other noble gases, molecular propellants and condensable elements. Such propellants offer certain advantages in terms of specific mission scenarios, or for certain propulsion system sizes. This paper represents a review of alternatives to the conventional xenon propellant for Hall thrusters, providing a comparative study of the most feasible alternatives. Various considerations of using alternative propellants are outlined, and a comprehensive database of experimentally measured Hall thruster performance is compiled to pair the measured performance using various propellants to the results of a theoretical propellant performance estimation.

1. Introduction

Of the many different electric propulsion systems developed for satellites, currently the Hall thruster is the most popular. It combines a high specific impulse, typically 1000 to 3000 s depending on the input power [1], with a high thrust to input power ratio. Relative to gridded ion thrusters, which typically possess a higher specific impulse, Hall thrusters intrinsically have approximately twice as greater thrust output at a given power. Xenon is typically used as the propellant of choice within Hall thrusters. It is an inert, heavy element that possesses a high ionization cross section and the lowest first ionization potential of the stable noble gases, along with the highest storage density when stored under pressure. Hall thrusters possess a significant flight heritage dating back almost fifty years, and span several orders of magnitude in terms of size, from 40–50 W up to 50 kW and above. Coupled with advances in magnetic shielding, which significantly increase the Hall thruster lifetime, these advantages have led to Hall thrusters recently becoming the high performance electric propulsion system of choice across a wide variety of different spacecraft missions [2].

Hall thrusters are now employed in scenarios ranging from orbit raising propulsion systems for microsatellites [3], to primary propulsion system for geostationary satellites [4], and even for interplanetary missions [5]. In terms of their use on microsatellites, various small satellite constellations are being deployed using Hall thrusters. This includes the SpaceX Starlink constellation (approximately 12,000 satellites, with 3200 deployed and operational as of December 2022) [6], OneWeb (648 satellites, with 462 deployed as of February 2022) [7], the Amazon Kuiper constellation (3236 satellites, first launch in mid 2023) [8], and many others (Astranis, AST SpaceMobile, Omnispace, Telesat). The majority of these satellites require changes to the semi major axis after launch vehicle deployment, with most requiring a significant attitude increase. Furthermore, strict de-orbiting requirements are enforced leading to additional propellant mass. Assuming a total xenon load of approximately 4.5 kg per satellite unit for station keeping and de-orbiting requirements, the subsequent xenon consumption per fleet becomes significant. Geostationary satellites with all electric propulsion systems are further increasingly adopting Hall thruster technology (Airbus Defence and Space and SSL). An average all electric geostationary satellite that utilizes Hall thruster propulsion units weights on average 1–3.5 tonnes carrying on board a total xenon propellant load of approximately 0.2–0.4 tonnes [9,10]. Other applications include the Lunar Gateway where it is envisaged that four 12.5 kW

* Corresponding author.
E-mail addresses: V-G.Tirila@soton.ac.uk (V.-G. Tirila), alain.demaire@ohb-sweden.se (A. Demairé), C.N.Ryan@soton.ac.uk (C.N. Ryan).
[1] Ph.D. Student.
[2] Propulsion BD.
[3] Associate Professor.

https://doi.org/10.1016/j.actaastro.2023.07.047
Received 18 December 2022; Received in revised form 10 June 2023; Accepted 31 July 2023
Available online 4 August 2023

Hall thrusters will be used, with a total xenon throughput of approximately 5 tonnes [11]. Further, low thrust interplanetary missions, which have previously used gridded ion thrusters almost exclusively, are also adopting Hall thrusters. The eponymous Psyche mission to a metallic asteroid will use an SPT-140 Hall thruster with a total throughput of xenon of 1.03 tonnes [12]. Constellations have increased the total number of satellites deployed in orbit from a few hundreds to over a thousand per year [13,14] demonstrating an exponential growth. Assuming a similar growth pattern, total satellites deployed would increase from 389 in 2019, 1202 in 2020, 1778 in 2021 to over 4000 by 2026. If all of the satellite units in the Starlink, OneWeb, and Amazom Kuiper constellations used xenon propellant (assuming 40% of the total number of satellites launched over the next 5 years), together with the larger geostationary satellites and unique spacecraft missions which use over 1.5 t of propellant (assuming 1% of the total over 5 years) then as a minimum the total xenon expenditure would exceed 260 tonnes of xenon.

The world production of xenon per year grew from 30–40 tonnes in 1998 [15] to 53 tonnes in 2015 [16]. Xenon is extracted as a byproduct of the cryogenic oxygen and nitrogen extraction through air separation [17] with a limited total output dependent on the available xenon concentration in air [18]. As a result of extensive use of xenon in other major industries such as an anaesthetic agent [18] or part of automotive lighting systems, xenon availability and price are in constant fluctuation [16]. Recent global events such as the COVID-19 pandemic and the Russia–Ukraine war have further significantly disrupted the supply chain and availability of rare elements such as xenon [19] driving a major increase in price. Consequently, in the global context there is a high risk of shortage for xenon. In this context procurement of large quantities of xenon (>3 tonnes) is likely to be unfeasible and at risk of drastically affecting the already volatile cost unless spread out carefully over several years.

Xenon usage for spacecraft electric propulsion applications accounted to approximately 10% of the xenon demand in 2015 [16] while current market studies suggest a 30% share of the total xenon demand dedicated to electric propulsion satellite usage [20]. Given this limitation of tens of tonnes of xenon available per year and a ceiling limitation on total xenon production [18], an increase in future users of xenon propelled electric propulsion enabled spacecraft will put significant strain on the supply. Combined with users from a wide range of industries, and also other spacecraft missions, a search for a sustainable alternative to xenon as a propellant becomes justified in the context of the rapidly expanding electric propulsion sector.

Various other propellants have been investigated for Hall thrusters, which can be categorized in three groups: gaseous propellants, condensable propellants, and molecular propellants. Gaseous propellants include monoatomic noble gases such as xenon, krypton, argon, and neon. Condensable propellants, defined in short as propellants which are either solid or liquid at or near room temperature, include metals such as bismuth, zinc and magnesium [21–24], but also other options such as iodine [25]. Thirdly there has been growing research interest in using molecular propellants such as tertiary amines [26] but also other gases such as carbon dioxide, oxygen and nitrogen, in particular within the scope of air breathing electric propulsion [27]. Across this wide selection of different alternative propellants each has particular advantages and disadvantages, depending on their elemental properties, ionization abilities, and measured performance.

This paper evaluates the use of alternative propellants within Hall thrusters, providing a review of current alternatives investigated, through a comprehensive database of experimentally measured performance values. Further considerations such as ionization, storage density, and condensable propellants heating requirements, are analyzed. Through a comparison to a predictive performance law for different propellants at different powers, possible alternative propellant replacements for xenon are identified for low power Hall thrusters (broadly relating to mega constellation requirements), medium power Hall thrusters (broadly relating to geostationary satellites), and high power Hall thrusters (for future applications such as interplanetary missions).

2. Gaseous propellants

2.1. Krypton

Krypton is currently the most widely used alternative to xenon in Hall thrusters both in in-space hardware, demonstrated by the use of krypton in the Starlink constellation, as well as in ground testing. Krypton offers several similar traits to xenon; it is chemically inert, gaseous at ambient conditions, and benefits from simple handling procedures. The major benefit of krypton is that it is available at a significantly lower cost than xenon, approximately five times less expensive, and it can be tested with existing electric propulsion hardware including power processing units and hollow cathodes. Krypton has been used extensively in Hall thrusters across a wide variety of input powers, from sub kW to medium power Hall thrusters, to 10's kW Hall thrusters [1, 28–34].

There are however various disadvantages associated with krypton, in particular under typical tank pressures its storage density is approximately a third that of xenon. Krypton is 64% lighter than xenon, and so the theoretical thrust-to-power ratio will be lower for krypton fed thrusters at 79.8% of the equivalent power xenon ratio. However, the lower mass krypton can produce 25% higher Isp than xenon, although the effect may only be apparent at high discharge powers where the thruster is operating efficiently [1]. It has been observed that krypton has a significant reduction in efficiency, explained for the most part by a reduced mass utilization and beam current utilization efficiency [1, 28,36]. This has been further corroborated in more recent studies focusing on lower power Hall thrusters [30,33]. These effects can be understood through the slower ionization process resulting from the combination of a small cross sectional area, faster thermal velocity, and higher first potential for ionization. Various studies have investigated mitigating methods against the lower performance, through the variation of the magnetic field profile [32], or the injection of the krypton in a rotating rather than axial manner [31]. These promising results suggest there may be methods of increasing the thruster efficiency.

Krypton has been extensively tested in Hall thrusters across all power levels, with particular interest in thrusters operating at higher powers where xenon use is very costly. A database of available performance data was compiled for Hall thrusters utilizing krypton and xenon and their relative performance as propellants is shown in Figs. 1 2 3. It must be noted throughout the study that a Hall thruster designed and optimized for a particular propellant will perform differently when

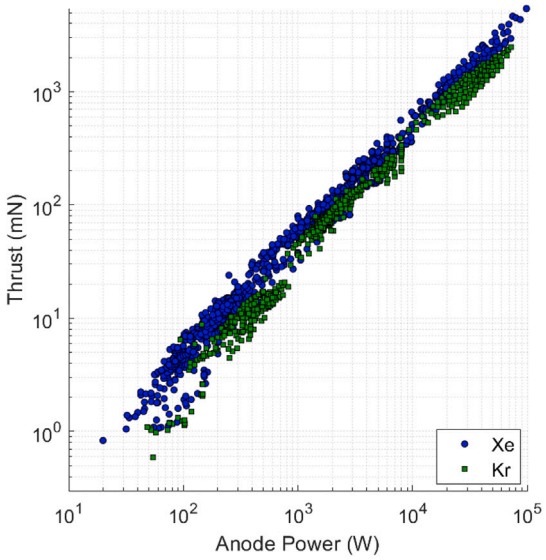

Fig. 1. Thrust vs anode power for Hall thruster operating on xenon and krypton.

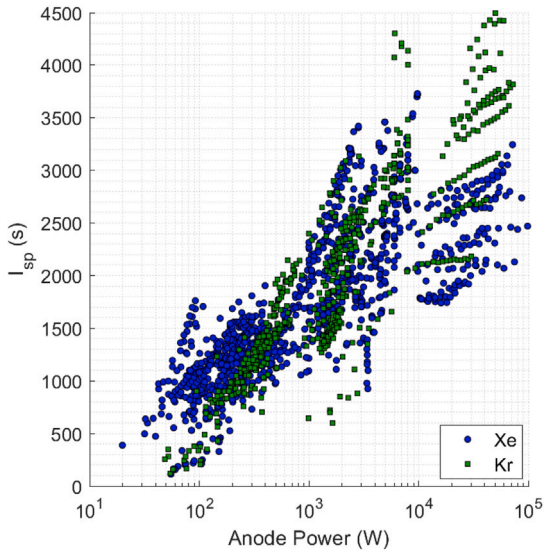

Fig. 2. Specific impulse vs anode power for Hall thruster operating on xenon and krypton.

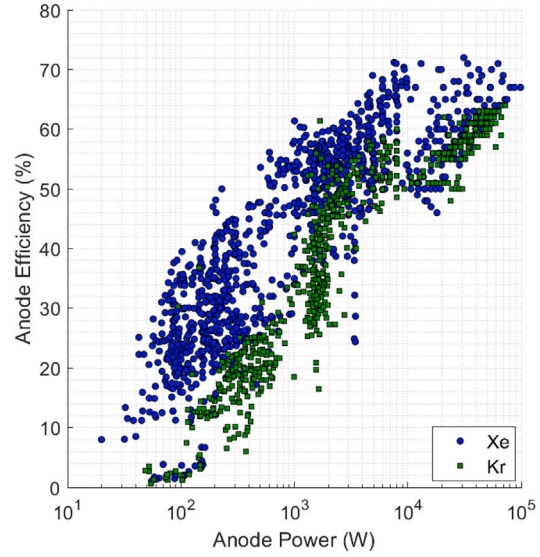

Fig. 3. Efficiency vs anode power for Hall thruster operating on xenon and krypton.

operated with a different propellant [37]. More than 50 unique Hall thrusters at multiple operating conditions are featured in the dataset to highlight the general propellant behavior and performance trend. Propellant centric design and refinement of the Hall thruster may increase the performance beyond the trends observed in the dataset [1].

Due to the small atomic mass, krypton fed Hall thrusters produce less thrust at the same power level. However, as the discharge power exceeds kW levels, krypton is shown to produce a higher specific impulse than xenon at similar power levels. In high power thrusters above 10 kW (NASA-173Mv1, NASA-173Mv2, NASA-457M, X-3), krypton specific impulse is much higher than xenon. However, this does not equivalently translate into a high anode efficiency as krypton fed Hall thruster data show poor performance at over 20% lower efficiency in sub kW class thrusters and a 5%–10% lower efficiency above 10 kW in direct comparison to xenon at the same power level. Recent results show that the efficiency penalty may be averted in high current density scenarios [38] where krypton may exceed xenon performance.

Krypton remains a useful propellant alternative for Hall thruster systems due to the low cost, ease of use, and low risk associated with it making it well suited for system testing and development. However, as a viable alternative for xenon for in-space applications with Hall thrusters considerable work remains to be done. High-Isp missions may benefit from the 25% higher Isp offered by krypton, but it remains severely limited by the impact on mission lifetime as well as the low storage density possible.

2.2. Argon, neon and helium

Since the initial development of Hall type thrusters various light propellants have been investigated. Early research focused on the use of light noble gases such as helium [39], argon [40,41] with xenon use investigated later [42]. Argon usage as a propellant was proposed due to its low cost and inert qualities. Usage of argon in Hall thrusters has been readily demonstrated yet performance data in direct comparison to xenon is scarce [35]. Although stable operation was achieved, performance of argon as a propellant is poor compared to xenon and krypton. However, the recent use of argon in Starlink satellites was reported to have high efficiency exceeding 40%, yet no technical studies have been publicly released at this time. Data for the THT-VI thruster [35] operating on pure argon is shown in Fig. 4 highlighting the performance trend of argon. Peak anode efficiency is found to lie below 10% offering moderate thrust and specific impulse performance. A major disadvantage of argon is also the low density even under pressurized conditions (approximately 16% of the total density of xenon at the same pressure) which makes it undesirable for in-space operation. In addition the low atomic mass, density and worse ionization requirements lead to a high flow rate associated for sustained thruster operation. This limits significantly its use in ground testing depending on the pumping facilities used.

Other light monoatomic inert propellants such as neon or helium will likely suffer from similar issues in terms of ionization characteristics, volumetric requirements, and ultimately reduced efficiency [35].

2.3. Gas mixtures

An important property of gases is their ability to mix with each other. This opens up the possibility of propellant mixtures being used in Hall thrusters to offset the high cost of pure xenon or reduce the efficiency deficit of krypton and other lighter propellants.

Various studies have investigated the use of mixtures of xenon and krypton for Hall thrusters. Promising initial results were demonstrated showing a high anode efficiency at a high power when using a krypton/xenon mixture [43]. Plume measurements demonstrated an increase of the beam divergence with higher krypton percentage (>50%) in the propellant mixture [44]. Similarly, the thrust efficiency decreases when the krypton fraction is increased [44,45]. Yet it was shown that a small reduction in xenon percentage (75% xenon/25% krypton) does not drastically impact performance [44].

Other studies have investigated argon/xenon mixtures [35,46]. In this case it was demonstrated that the relatively low argon efficiency can be increased through a higher xenon percentage (>40%) and through channel geometry modifications that improve argon ionization [46]. It was also shown that a low argon percentage does not significantly impact performance enforcing similar results to krypton mixing.

Currently, research is focused on mixing molecular propellants such as carbon dioxide and argon or nitrogen, oxygen and argon in order to recreate atmospheric conditions particularly in the interest of adopting air-breathing propulsion [35,47,48]. Thruster performance was demonstrated on these mixtures reaching an operational anode efficiency of 27% [48] with further work underway. Due to the complex nature of mixed propellant behavior and the scarcity of performance data, this study does not analyze them further.

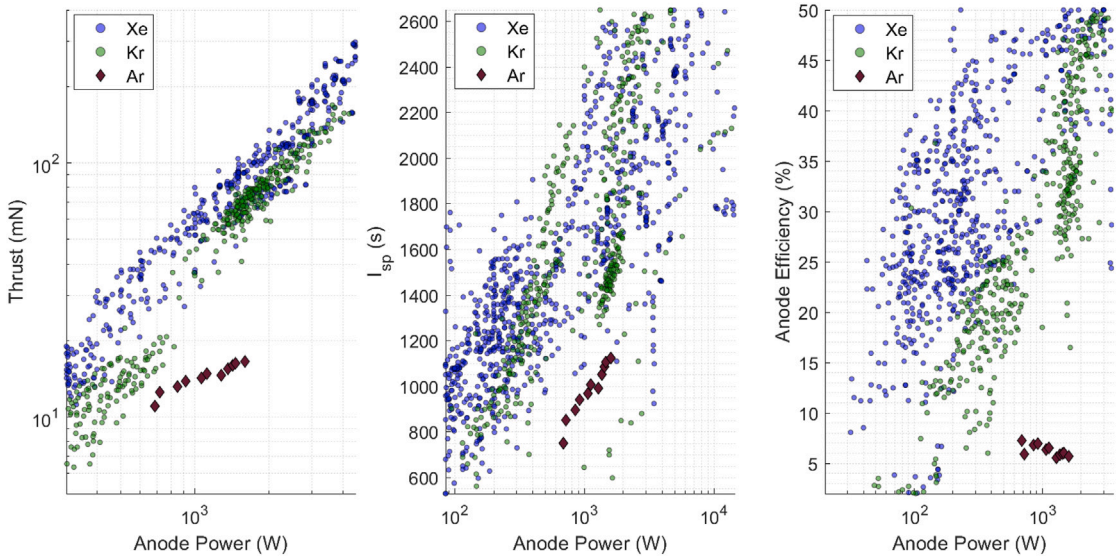

Fig. 4. Thrust, specific impulse and efficiency vs power for Hall thrusters operating on [35].

3. Condensable propellants

The second category of propellants that can be defined are condensable propellants. Elements in this category produce a high enough vapor pressure when heated at low ambient pressure to drive a gaseous flow through either a feed system or directly in the discharge chamber, providing a propellant in gaseous form which can then be ionized. Without heat input, the propellant reverts to the initial phase through condensation. Condensable propellants considered are mostly solid elements such as iodine [25,50,51], bismuth [22,52,53], zinc and magnesium [21,23,54], but also metals found in a liquid state near ambient conditions, such as caesium and mercury [55–57]. Table 1 summarizes the physical characteristics of condensable propellants that have been investigated, with xenon and krypton included for comparison.

A short introduction to propellant heating and transport follows for the purpose of defining the individual limitations of condensable propellants. An investigation into the usage considerations and performance in Hall thrusters for each element is then presented.

3.1. Heating power penalty

Unlike gaseous propellants condensable propellants require additional thermal energy to phase change. This can be considered the power penalty associated with condensable propellants usage, which should be estimated for a fair comparison with gaseous alternatives. We present a simplified investigation into the achievable vapor pressure p_V of an element at a specific heater power input.

A variety of equations may be used to relate vapor pressure to the temperature of the propellant as a result of sublimation/evaporation including the Clausius–Clapeyron equation, Antoine equation, or other empirical estimations dependent on the element of interest [58,59]. Propellant vapor pressure equations are described as a function of propellant temperature constructed with element specific coefficients derived from experimental data. The Antoine equation is presented as an example of such an equation [58]

$$\log p_V = A - \frac{B}{C+T}. \tag{1}$$

where A, B, and C are substance and phase specific coefficients. In this study, the Antoine equation is used to represent iodine data [60]. However, not all the propellants presented fit the template of Eq. (1). Consequently, the vapor pressure curves of bismuth, zinc, magnesium and cadmium are described by other empirical relations [53,61].

Vapor pressures curves for a selection of condensable propellants are illustrated in Fig. 5. The resulting vapor pressure for different elements varies by several orders of magnitude at one target temperature. Bismuth, magnesium, zinc and cadmium show a slow to moderate vapor pressure increase with temperature while iodine exhibits a high vapor pressure increase at low temperature increments. Data in Fig. 5 show that cadmium and zinc present a similar temperature–pressure behavior with a relatively low peak vapor pressure (15 Pa and 21 Pa, respectively) at their melting points (321.1 °C and 419.5 °C, respectively). Magnesium can achieve a much higher vapor pressure whilst still in solid form (390 Pa), before reaching its melting point (650 °C).

Iodine presents the highest vapor pressure (>23 kPa) out of all the condensable propellant options at a very low temperature input (up to 120 °C).

Bismuth can achieve a significant vapor pressure (20 Pa) only above 800 °C past its melting point (271.4 °C).

It is important to also note the lower end of the vapor pressure–temperature curve. This shows that cadmium, zinc, magnesium and

Table 1
Physical properties of several previously investigated propellants for Hall thrusters. *Data at 14 MPa, 50 °C, from NIST database. [21,49].

	Xe	Kr	I	Mg	Zn	Bi	Cd	Hg	Cs
Mass (u)	131.3	83.8	126.9	24.3	65.4	209	112.4	200.6	132.9
Ionization Properties									
First ionization energy (eV)	12.1	14	10.5	7.6	9.4	7.3	8.9	10.4	3.9
Peak cross section (Å^2)	4.8	3.7	6	8	5	8	–	8.3	9.4
Storage and Handling									
Density STP (g/cm3)	1.6*	0.5*	4.9	1.7	7.1	9.8	8.7	13.5	1.9
Melting point (°C)	−112	−157	113.7	650	420	271	321	−39	28
Vapor pressure at melting point (Pa)	–	–	2.34e+4	384.01	21.49	7.5e−3	15.34	–	–
Toxicity/difficulty to handle	–	–	Med.	Med.	Low	Low	High	High	High

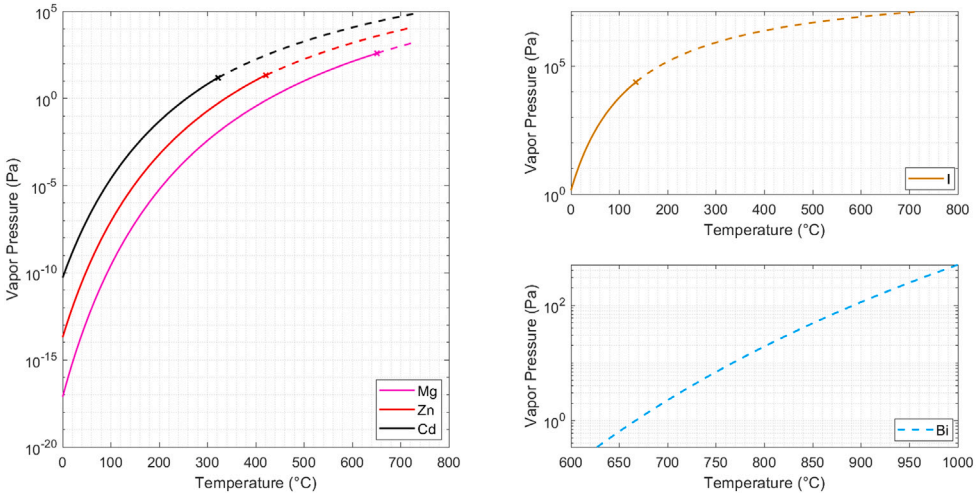

Fig. 5. Vapor pressure versus temperature for a selection of Hall thruster solid propellants. Propellant phase: solid — solid line; liquid — dashed line; Vapor pressure equations and coefficients sourced from: Mg [61]; Zn [61]; Cd [61]; Bi [53]; I [60].

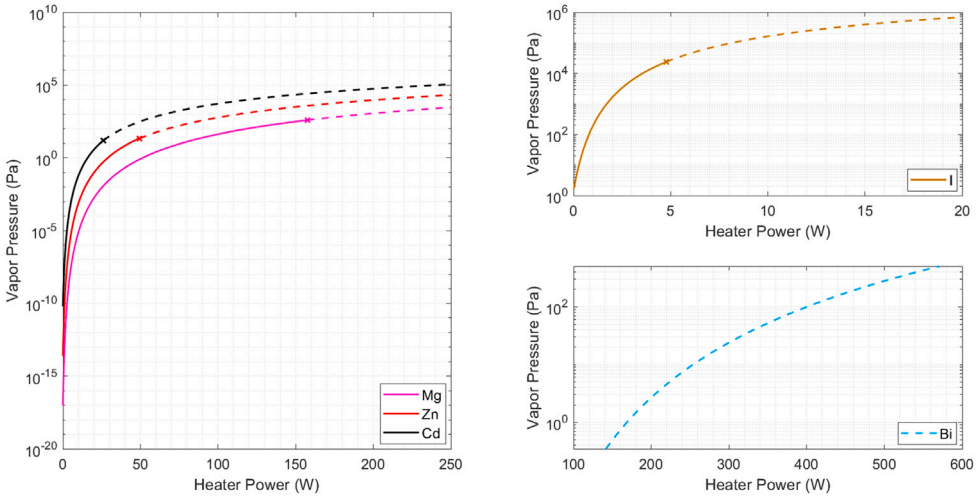

Fig. 6. Vapor pressure curves for solid propellants versus estimated heater power. Propellant phase: solid — solid line; liquid — dashed line; Vapor pressure equations and coefficients sourced from: Mg [61]; Zn [61]; Cd [61]; Bi [53]; I [60].

bismuth will not significantly sublimate (vapor pressures lower than 10^{-5} Pa close to 100 °C) unless heated above an element specific temperature threshold (for Cd ≈ 210 °C; Zn ≈ 280 °C; Mg ≈ 370 °C; I_2 ≈ 0 °C; Bi ≈ 610 °C) which suggests that condensation on unheated surfaces will not act as a secondary sublimation site for cadmium, zinc, magnesium and bismuth. Iodine on the other hand can produce more than 30 Pa at 25 °C which implies a higher likelihood of secondary propellant sublimation upon surface condensation, increasing the risk of contamination propagation.

In essence, a certain surface temperature leads to a consequent sublimation rate hence a vapor pressure (Eq. (1)). To maintain the surface at a required temperature a certain amount of energy is required to balance the heat losses. Assuming radiative heat loss from the surface of the propellant as the dominant loss mechanism, independent of propellant tank design, and discarding conductive losses and phase change losses which would vary depending on the system architecture, vapor pressure can be tied to heater power required to maintain the surface temperature balance through the application of the Stefan–Boltzmann law

$$P = \epsilon\sigma A(T_s^4 - T_{amb}^4). \tag{2}$$

The advantage of this simplified approach is that it is propellant centric and as a result removes the influence of the storage and delivery architecture allowing a peer to peer comparison of propellants. Using a fixed average emissivity value of $\epsilon = 0.15$ (corresponding approximately to a machined metallic surface) and an arbitrary sample surface area of $A = 0.025$ m^2 (equivalent to a square surface with a side length of 15.8 cm, representing a relatively small propellant tank suitable for a thruster in the 100 W–1 kW power class), vapor pressure versus input power curves can be drawn for selected elements as shown in Fig. 6. The most power efficient condensable propellant is iodine requiring approximately 5 W to produce a very high vapor pressure > 10^4 Pa at this scale. Cadmium and zinc require a higher input power; more than 26 W and 50 W respectively to achieve an exploitable vapor pressure of approximately 20 Pa. Given its high melting point, magnesium can operate at a much wider power interval from 85 W to 150 W, producing a higher vapor pressure than zinc and cadmium. Finally, bismuth requires upwards of 300 W to sustain a vapor pressure of more than 20 Pa at this scale.

Experimental results are presented to acknowledge the capabilities and limitations of this analysis. Low powers Hall thrusters (50 W–200 W) operating on iodine required between 5 W to 10 W to sublimate the propellant and sustain operational vapor pressure within the tank [62–64]. Zinc, experimental data suggest that between 30 W

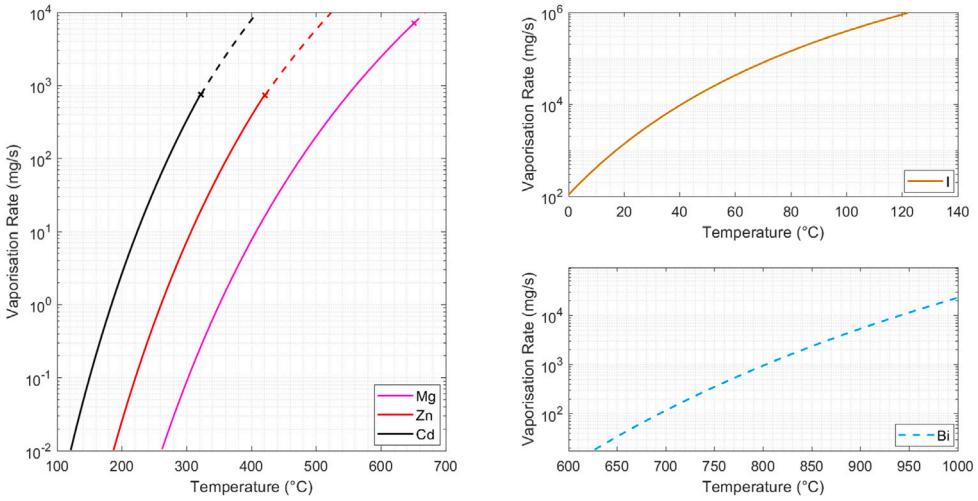

Fig. 7. Sublimation/evaporation curves for solid propellants versus temperature. Propellant phase: solid — solid line; liquid — dashed line; Vapor pressure equations and coefficients sourced from: Mg [61]; Zn [61]; Cd [61]; Bi [53]; I [60].

to 50 W were needed for the propellant tank to sustain the flow rates required by a 100 W thruster [65,66] through sublimation. Hall thrusters operated on magnesium (1–2 kW) required 100–600 W for the heater while higher power thrusters (2–3 kW) required 500–1.2 kW heating power [67]. Bismuth evaporation data is scarce, with some reports suggesting a few kilowatts of power required for propellant vaporization and transport (for a >100 kW thruster) [68] while others state an estimate of >150 W (for a 25 kW thruster) [53].

While low power Hall thrusters show some agreement with the predicted heating power requirements derived in Fig. 6, higher power thrusters are more sensitive to system level losses. Propellant can phase change in the heating process resulting in a considerably higher emissivity [69], that leads to higher radiative losses. Input heater power is heavily influenced by the mass of the propellant, exposed propellant area and propellant storage and delivery system architecture since the propellant storage in turn suffers heat loss through radiation and conduction increasing losses in larger thrusters.

In many cases sublimation/evaporation of a condensable propellant occurs externally in a propellant tank and as a result the gaseous propellant must also flow to the discharge chamber through a feed system, incurring additional losses that impact the input heater power. The flow transport characteristics of condensable propellants are discussed in the following section.

3.2. Propellant transport

The Hertz–Knudsen equation can be used to predict the mass flow rate resulting from sublimation/evaporation from a free surface. Assuming that the distribution of gas particle velocities is Maxwellian and that particles do not interact with each other, the flux of gas particles from a surface is given by [70]

$$\frac{\dot{N}}{A_{open}} = \frac{p_V}{\sqrt{2\pi M k_0 T}}, \tag{3}$$

where $\dot{N}$ is the flow rate of particles, A_{open} the area of the evaporating surface, and M the mass of the particles. Accounting for ambient pressure and converting from particle flux to mass flow rate, the mass flow rate of sublimated/evaporated propellant from a free surface is

$$\dot{m}_s = \frac{(p_V - p_{amb})A_{open}\sqrt{M}}{\sqrt{2\pi k_0 T}}. \tag{4}$$

For a constant ambient pressure and surface area, the sublimation/evaporation mass flow rate depends on propellant temperature as shown in Fig. 7. A similar trend to the vapor pressure curves is expected and observed. Using Eq. (4) high propellant sublimation/evaporation rates are achievable with every condensable propellants.

In the particular case of an exposed anode built from the propellant material this mass flow rate becomes the direct propellant injection rate, a design successfully investigated by Michigan Tech. [23]. However, the derived evaporation/sublimation mass flow rate is a misleading factor when considering other propellant feed systems that do not sublimate/evaporate directly in the discharge channel. Many propellant delivery systems using condensable propellants include relatively small pipework between the propellant tank, where the propellant sublimation/evaporation generally occurs, and the thruster channel [21,51,64,71]. This can lead to constriction of gas flow, and a reduction in the actual mass flow rate achieved. Using the Darcy-Weisbach equation a simple propellant transport mass flow rate estimation through a conventional circular feed can be expressed with the following form

$$\frac{\Delta p}{L} = f_D \cdot \frac{\rho v_m^2}{2D}, \tag{5}$$

where Δp represents the pressure difference between the saturated propellant vapor and the ambient conditions, L and D the length and diameter of the feed, v_m the mean flow velocity and f_D the friction factor which can be regarded as a function of the Re number. Introducing the transport propellant flow rate as a function of mean velocity, the equation can be rearranged to give

$$\dot{m}_t = \pi\sqrt{\frac{\rho \Delta p D^5}{8 L f_D}}. \tag{6}$$

Within this equation the most important parameters are the pressure differential, the feed system dimensions and the friction factor.

In the particular case of iodine, the pressure differential is very high (>10^4 Pa) at a low power input (5 W) in vacuum conditions (Figs. 5 and 6). Therefore, iodine functions in a similar manner to a pressurized propellant, with no flow rate limitation due to pipe frictional losses. This helps to make iodine widely suitable across different thruster sizes (with varying associated flow rates).

Other condensable propellants (Mg, Zn, Cd, Bi) require a higher power input to produce an exploitable pressure differentials (Fig. 6). In an effort to minimize power it is desirable to operate at the lowest possible propellant vapor pressure for transport. Yet at this point, the feed dimensions and friction factor may become flow restrictive.

The cross-sectional area of the feed system is the most important factor at facilitating propellant transport, and hence at reducing required heater power. The diameter of the feed system can be maximized

and the length of the feed reduced to improve the gas phase flow transport rate according to Eq. (6). However, this method is limited by the size of the thruster and its components such as anode and discharge channel, specifically its diameter and height. This further implies a thruster size limitation with certain propellants. For example, in a small 100 W Hall thruster with a 5 mm discharge channel height, the annular anode width calculated from the outer–inner diameter difference cannot exceed 5 mm. As the main propellant distribution point, the anode connects to the propellant feed. Consequentially, the anode feed diameter cannot exceed the 5 mm height of the thruster discharge channel in a conventional design imposing a limit on the D term in Eq. (6). Multiple propellant feeds can be connected to the anode to partially overcome this phenomenon, however the number of propellant feeds connected to the anode distributor is still bound by the limited small dimensions of the thruster. With a thruster size limit on the diameter, other parameters become important in propellant transport.

The friction factor f_D has a strong dependency on the Reynolds number, with values > 5 (when $Re < 10$) to < 0.005 ($Re > 10^8$) [72–74]. In a laminar, low speed circular pipe flow, the friction factor may be estimated based on a simple Reynolds dependency [73]

$$f_D = \frac{64}{Re}. \tag{7}$$

In other flow regimes, the friction factor relates differently to the Reynolds number yet still holds its strong dependency [72–74]. Subsequently, the Reynolds number is defined as the ratio of inertial forces to viscous forces

$$Re = \frac{\rho u D}{\mu}. \tag{8}$$

With a lower Reynolds number, viscosity is more prevalent consequently increasing the friction factor by a few orders of magnitude. In the limit case of continuum laminar flow at low Re ($Re < 10$, $f_D > 5$) a viscosity estimation for the propellant becomes important. This is because in a fixed feed diameter case, the viscosity–friction factor dependency may inhibit transport at a minimum pressure differential (which is the most desirable operation point for power efficiency) resulting in a higher power draw to increase the pressure differential to overcome the effect.

We further estimate the viscosity of condensable propellants gas phase to assess which elements are more prone to propellant transport issues at lower thruster scales and input heater power. In the absence of other experimental data, viscosity can be estimated using the following equation [75]

$$\mu = \frac{16.64T\sqrt{M}}{\sigma^2\sqrt{\epsilon/k}}, \tag{9}$$

where T represents the gas temperature, M represents the molecular mass, σ the collision diameter of the element and ϵ/k is the Lennard-Jones depth of potential-energy minimum [76].

The resulting viscosity estimation is shown in Fig. 8 for the most likely operational temperature range of each propellant. Heavier elements such as bismuth, cadmium and zinc are more viscous at operational temperatures, therefore more resistive to transport at a low pressure differential required to minimize power. Experimental observations with zinc show that propellant transport is difficult at low vapor pressure due to viscous effects [65,66]. Elements such as magnesium and iodine present a lower viscosity and higher vapor pressure facilitating transport at most temperatures.

The viscosity of the condensable propellants studied is higher by an order or magnitude or less compared to other gasses such as xenon or krypton at normal conditions of temperature and pressure. Consequently, the resulting friction factor can vary by two orders of magnitude in the case of condensable propellants with a cascading effect on propellant transport flow rates.

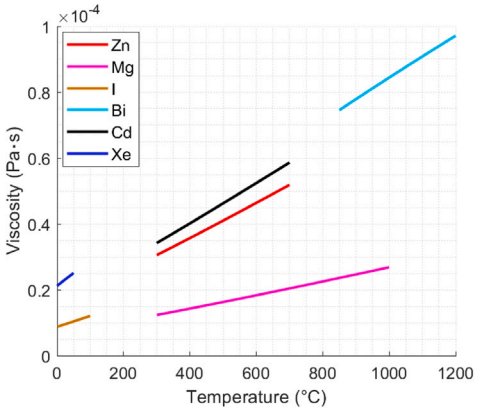

Fig. 8. Viscosity versus temperature for gas phase elements in their respective operational temperature range.

Therefore, the resistive effect of viscosity is limited but not negligible in estimating a propellant power requirement. Propellant transport is further complicated by the local or global flow regime changes within the geometry of the feed system. A Knudsen number analysis coupled with a feed architecture specific flow model is critical in optimizing the power expenditure in condensable propellant usage.

3.3. Propellant storage and delivery

Although condensable propellants are mostly solid at normal temperature and pressure as highlighted by Fig. 6, the propellant phase may change during the heating process, if higher pressure differentials are required (with the exception of iodine). This affects the design of the storage and delivery system. Propellants such as iodine and magnesium can be used in solid form with the production of gas phase propellant through sublimation while zinc, cadmium and bismuth are most likely to become liquid at operational temperatures producing the gas phase propellant through evaporation. Sloshing, uneven heating and filter permeation may become important concerns with operation on a liquid phase propellant.

A variety of propellant storage and delivery solutions have been developed for condensable propellants [21–23,51,66]. Among them, two broad design categories can be identified based on the location where the gas phase propellant is generated.

The first category can be defined as localized evaporation/sublimation at the anode. In this case, a heated anode is made out of the propellant itself with the propellant/anode undergoing direct sublimation in the discharge chamber during thruster operation [23,54] (Fig. 9). The major advantage of the system is minimal heater power usage as the propellant is heated by the discharge, reducing significantly the power requirements for gas phase generation. The main limitation lies in the reduced volume of propellant that can be held within the discharge channel of the thruster. Alternatively, liquid phase propellant can be fed to a porous heated anode which evaporates the propellant in the discharge chamber [22,53] (Fig. 10).

This method is more suitable for propellants where the required sublimation/evaporation rate is above the melting point of the propellant. Bismuth is the best example for this design approach as the propellant bulk, held within the delivery system, can be heated at 280 °C just above the melting point, and fed in liquid state to the anode, which evaporates the bismuth at 1000–1200 °C. This is more energy efficient than heating the bulk propellant and the feed system together at 1000–1200 °C. The main disadvantage of the system is the need for a propellant delivery system that can operate at high temperature, either using pressurized gas [22] or electromagnetic pumps [53].

The second category can be defined by external (tank) evaporation/sublimation and propellant gas phase transport to the anode [21,

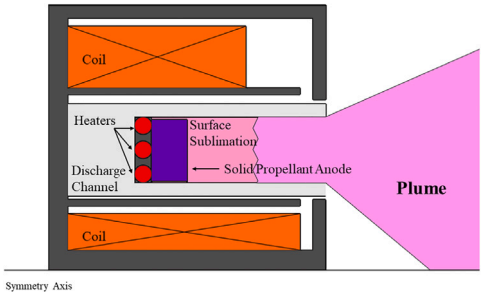

Fig. 9. Solid anode propellant delivery system.

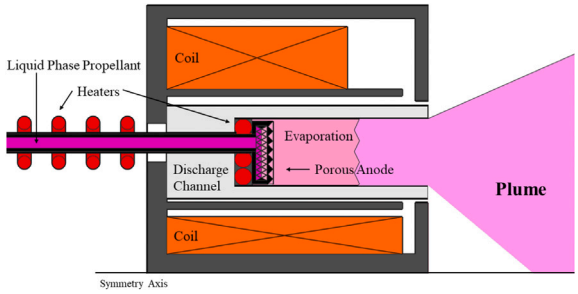

Fig. 10. Porous anode propellant delivery system.

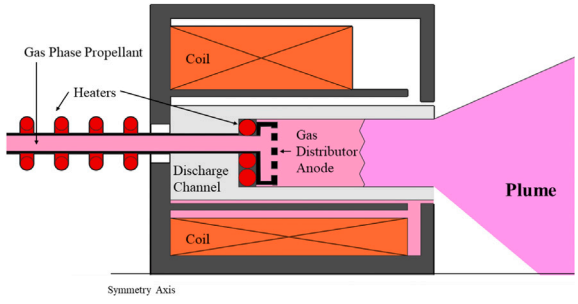

Fig. 11. Gas distributor anode propellant delivery system.

51,64] (Fig. 11). External tanks have been commonly used with smaller amounts of propellant and also with lower operating temperature propellants [51]. This system is used mostly with iodine where gas phase generation is very cheap from an energy point of view (5–10 W needed for $>10^4$ Pa), resulting in a need for an additional flow control system for the high pressure vapor [71,77,78]. For flow control, thermal throttles [71], a controlled geometric restriction [77], or a heated standard flow controller has been used. The external tank design is suitable for use both with sublimating propellants [66], or liquid-propellant containing tanks that feed propellant vapor [21]. The disadvantage of the system is the additional energy expenditure on feed line heating which must be maintained above the melting point of the propellant to prevent deposition.

As a result the propellant storage and delivery system is dependent on the selected mission profile, spacecraft specifications and thruster class as well as the type of condensable propellant used. A review of the performance achievements and particularities of condensable propellants is presented next.

3.4. Liquid metal propellants — caesium and mercury

The first propellants used in electric propulsion were of a condensable nature. In the early 1960's Pinsley et al. [55] investigated the use of caesium as a propellant within Hall thrusters, a propellant of interest in gridded ion thrusters at the time. This study investigated Hall thrusters using both electron impact and contact ionization of caesium [40]. The caesium Hall thruster produced a maximum thrust of 78.3 mN at an I_{sp} of 1600 s and a peak anode efficiency of 40%. Caesium was further used in single and two stage anode layer thrusters resulting in an I_{sp} of 1500 s and 3000 s respectively [79]. Alternatively, contact thrusters were designed to operate with caesium exploiting ease of ionization upon contact with a charged tungsten electrode [80]. Gridded ion thrusters were the main platform for mercury development in the 1960s and 70s [81,82] which culminated with an in orbit demonstration on the SERT I and SERT II missions. Although it demonstrated successful operation, conductive mercury deposition between the accelerator grid plates caused a thruster failure in the SERT II spacecraft [83]. Between the 1960s and 70 s research was undertaken in Germany with Hall thrusters tested on mercury propellants [40]. Several mercury Hall thrusters were developed: HIT 4 (1970) with input power up to 2.5 kW with efficiency in the 30% range; HIT 2 (1972) input power up to 500 W and efficiency in the 32% range; HIT 3 (1973) with input powers ranging from 100 W to 500 W, with a peak efficiency of 45%.

Work/research on mercury and caesium ion thrusters discontinued in the mid to late 1970s. Mercury presents high toxicity [84]. Caesium is highly reactive and pyrophoric [85] making it a hazardous substance to store, transport and use in ground testing facilities. Mercury, caesium and their respective ions pose significant threat to the materials that make up the spacecraft due to their corrosive nature [86,87]. In thruster usage, the corrosive effects limit the lifetime and pose significant threats to contact components. In comparison xenon was found to be inert, easy to use, and unaffecting of spacecraft components, offering good performance. Consequently, xenon replaced mercury and caesium as the default propellant in electric thrusters, starting with the Meteor 6 satellite in 1971 [2].

3.5. Solid metal propellants — bismuth, magnesium and zinc

In the search for viable alternative propellants to xenon several metals have been suggested and investigated for use with Hall thrusters, in particular bismuth, magnesium, and zinc [21,23,88]. Other metals have been investigated, such as cadmium [89], but details are limited.

The wide range of physical properties exhibited by metal propellants is listed in Table 1. The variety in molecular mass and ionization characteristics suggests the most suited metal propellant may depend on the thruster power range, thruster size and mission scenario. Most metals possess a higher or equal density at ambient conditions to pressurized xenon, enabling a more optimal volume distribution within the spacecraft whilst eliminating the need for a pressurized tank. However, the propellant tank and feed system require heating to produce the gaseous phase ready for ionization and acceleration which represents their main drawback. The advantage of metallic propellant use is the financial savings associated with cheaper propellants, a more compact propulsion system that is not at the cost of a lower total impulse, and the availability of propellant for in-situ harvesting and usage.

As the largest non-radioactive element bismuth could potentially offer superior performance to xenon based thrusters. Its high mass results in a theoretically higher thrust-to-power ratio than is possible with xenon, which is beneficial for decreasing maneuver times and increasing payload mass [22,52]. From Table 1 it can be seen that bismuth offers very high storage density, six times that of xenon. The ionization properties of bismuth are also appealing, as it has both a low first ionization energy and a high peak ionization cross section. Bismuth provides significant economic advantages over xenon, with bismuth being approximately twenty times less expensive.

There are also significant disadvantages associated with bismuth as a propellant which make its use more appealing in large, high power thrusters. An inherent low vapor pressure incurs considerable power

expenditure towards heating the propellant in order to produce a functional gaseous mass flow rate suitable for a Hall thruster. Temperatures of more than 760 °C are required to obtain a vapor pressure above 10 Pa which also phase changes the solid bismuth into a liquid due to its low melting point of 271.4 °C (Fig. 6). The required parasitic power to heat the propellant and prevent condensation can be estimated using the analysis presented in this paper to exceed 150–200 W.

Consequentially, bismuth may be particularly suitable for high power Hall thrusters (above 5–10 kW), where the propellant heating will be a proportionally smaller power requirement. Developed in the 1970's in the USSR the TsNIIMASH D-160 Thruster with Anode Layer (TAL) Hall Thruster evaporated bismuth from a reservoir using ohmic heating of a thin walled molybdenum propellant tube. It operated between 20 kW and 140 kW at an anode efficiency of 70%, and produced an Isp of 4000–8000 s [68]. The VHITAL-160 thruster developed primarily in the United States in collaboration with the TsNIIMASH company was designed to improve upon the original bismuth thruster, and to bring the feed system closer to a flight ready model [53]. Bismuth was heated to liquid form to flow through the delivery system, and near the anode a heated porous carbon plug acted to vaporize the propellant. For both the D-160 and the VHITAL thrusters reports state that between 150 W to 1 kW of additional power was required for the vaporization of the bismuth propellant and to prevent condensation in the feed system [53,68]. Given the high temperature requirements of bismuth and the inherent low vapor pressure that incurs high heater power penalties, the feed system architecture is limited to a porous anode propellant delivery system with either a self contained bismuth reservoir or a liquid bismuth feed system. In both cases the thermal system power expenditure is high.

The contamination of the spacecraft by bismuth propellant is a significant concern. A study of potential impact of thin film deposition of bismuth on spacecraft surfaces identified that a bismuth thruster may have significant impact on the optical, thermal, and electrical properties of surrounding materials [90]. Several potential methods of mitigating these issues have been investigated, with the use of a simple shield seeming to be particularly effective [22,90,91]. However, thermal control of spacecraft surfaces is not a viable solution to prevent bismuth vapor condensation, given the high temperature that would be required to achieve a positive vapor pressure.

At the opposite end of the atomic mass spectrum, magnesium has been investigated as an alternative propellant for Hall thrusters [23,24,92,93]. The physical characteristics of magnesium are described in Table 1. Magnesium is a light metal (5.7 times lower density than bismuth and 8.6 times smaller atomic mass) with a high melting point whilst capable of producing vapor pressures of hundreds of Pascals, and with a significantly lower cost than xenon. Magnesium possesses a high ionization cross-section and a low first ionization energy level, making it efficient to ionize, although its low mass implies a high propellant velocity through the thruster channel which may decrease the ionization collision frequency. Theoretically high specific impulse is achievable, making magnesium an efficient propellant for the mid to high power thrusters. Magnesium is stored at a similar density to pressurized xenon, and requires temperatures of up to 600 °C to produce a relatively high vapor pressure > 100 Pa (Fig. 5). At these temperatures, the propellant is still solid with vapor created through sublimation, simplifying the propellant tank design and power requirements (50–60 W needed — Fig. 6). A much higher vapor pressure is achievable through evaporation after magnesium phase changes to a liquid at a considerably higher power input (>10^4 Pa at 100–150 W — Fig. 6). This behavior makes magnesium suitable for both medium power thrusters (1 kW and above) as well as high power thrusters (5–10 kW and above).

Magnesium has low toxicity and it is not considered to be hazardous to health. Magnesium however has a high reactivity. The high purity substance may spontaneously ignite on contact with air or moisture in powdered form producing toxic fumes. It can react violently with strong oxidants and other substances becoming a fire and explosion hazard if stored improperly. Natural MgO layer formation reduces the risk of reactivity in ground operations with solid magnesium being more stable than powder form. In spite of the inherent risk, usage in controlled conditions has not proven to be problematic in aerospace applications [94].

Some unique advantages of magnesium that have been considered in literature include the availability of magnesium in both Martian and lunar regolith [21]. This would potentially allow for the refueling of magnesium fed thrusters for further exploration or for a return journey with in-situ propellant processing. Secondly, due to its high reactivity, magnesium is also suitable for use as a fuel in chemical rockets, with a predicted specific impulse of above 200 s and 270 s when combined with CO_2 and H_20 respectively [95,96]. This could offer the possibility of a dual mode propulsion system.

Zinc is another high density metal that has been investigated as an alternative propellant for Hall thrusters, often in conjunction with magnesium [21,23,24]. A zinc atom is 2.7 times heavier than a magnesium atom, yet still half the mass of a xenon atom, and as such may be suited to missions requiring large changes in velocity, or those that are severely mass constrained. Zinc is stored as a solid at four times the density of xenon and magnesium, approaching the density of bismuth. The melting point of zinc at 419.5 °C is lower than that of magnesium at 650 °C. However, the achievable vapor pressure below the melting point is low at up to 21 Pa (Fig. 5). Coupled with the high viscosity of zinc, usage in solid form through direct sublimation is challenging [65,66]. Past its melting point > 10^3 Pa are achievable at 50 W input power (Fig. 6). This makes zinc a suitable propellant for medium power thrusters (1 kW and above).

Zinc is also more straight forward to ionize than xenon, as despite having a similar cross section of ionization the first ionization energy is approximately 25% lower. Zinc is also considered to be non-toxic with relatively low reactivity as a solid. It becomes more reactive in a powder form with water, sulfur, strong acids and bases, chlorinated solvents, amines and cadmium. In powder form, it can ignite in air, however it is generally stable in cool dry places [97]. Financially, zinc is one of the lowest cost metals at over 100 times less expensive than xenon [98].

Previous research targeted testing of zinc and magnesium in conjunction and as such the technologies tested are presented together. As with all solid metal propellants, significant challenges are faced in the design of the propellant feed system. Feed systems for zinc and magnesium have adopted a similar design to bismuth with a heated external tank that melts the propellant to maximize the available vapor pressure [21]. Other feed systems have used a zinc/magnesium wire feed in which localized heating of the wire end is used to produce the gaseous propellant [21]. Both of these systems allow for greater control over the mass flow to the Hall thruster channel, yet may involve a higher system complexity and heating requirements.

Similar to bismuth, direct evaporation of magnesium and zinc from a porous hollow anode has been investigated, as well as the direct usage of a machined zinc and magnesium anode [23,54]. The direct evaporation of a solid zinc anode was tested successfully. Thermal control was maintained using inert 'shim' electrodes placed within the channel, which served to intercept a fraction of the discharge current preventing run-away heating of the anode. This method provides a good measure of control over the anode heating and propellant generation [99].

An overview of the available performance data is shown in comparison to xenon and krypton data in Figs. 12 13 14. Overall, zinc magnesium and bismuth propellant performance data is scarce with few data points present. Thrust to power ratios of 49 mN/kW have been achieved in a Busek BHT-1500 Hall thruster at a discharge potential of 250 V with zinc while the specific impulse at 250 V, 1 kW was reported at > 2100 s [21]. A modified Aerojet BPT 2000 operating on magnesium achieved 34 mN of thrust at 200 V and 39 mN at 300 V with 1.7 mg/s of propellant. The specific impulse was reported at 2000 s for 200 V and upwards of 2700 s for 300 V. The anode efficiency

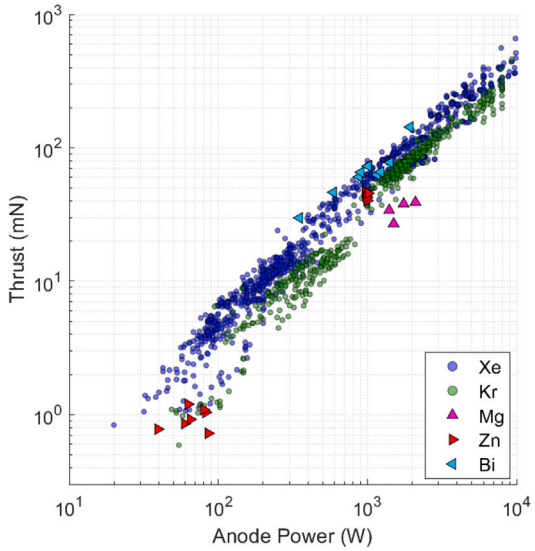

Fig. 12. Thrust vs anode power for Hall thruster operating on metallic propellants.

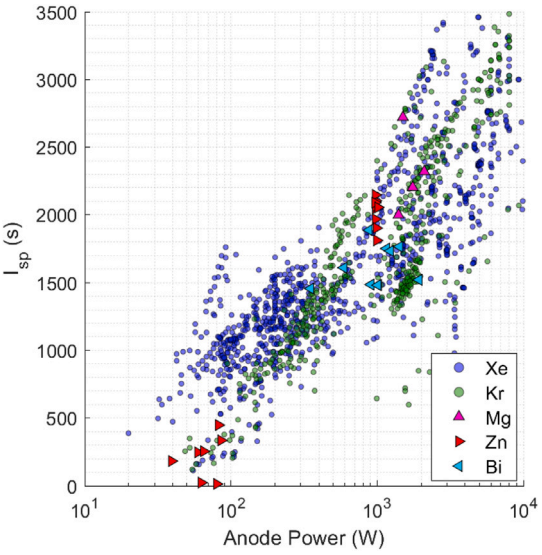

Fig. 13. Specific impulse vs anode power for Hall thruster operating on metallic propellants.

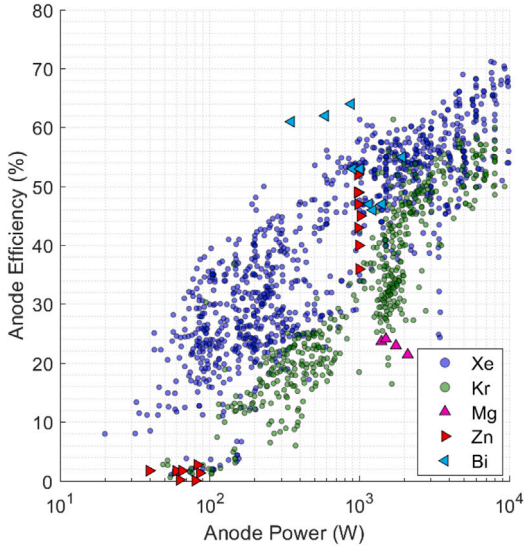

Fig. 14. Efficiency vs anode power for Hall thruster operating on metallic propellants.

was found to be 23% using magnesium which is substantially lower than the 40% anode efficiency of the thruster operating on xenon at approximately equivalent molar flow rates [24]. However, both thrusters used were designed specifically for xenon operation. Bismuth operation was also demonstrated by Busek on a modified BHT-1500 thruster. The measured thrust peaked at 73.4 mN at 1 kW discharge power. Maximum anode efficiency reached 64% at 880 W discharge power and 1888 s specific impulse [22]. At the same power level, bismuth outperforms xenon in terms of thrust and efficiency yet incurs significant power expenditure for propellant vaporization.

3.6. Iodine

The use of iodine as a propellant for both ion and Hall type thrusters was proposed in 2000 by Dressler et al. [100] and in 2001 by Tverdokhlebov and Semenkin [50]. Since then it has been the focus of considerable research and testing [25,64,101–103] with proven in-orbit demonstration on gridded ion thrusters [51]. This achievement follows substantial work in developing gridded ion thrusters and cusp field thrusters for iodine use [104–107].

Iodine can also be categorized as a molecular propellant since it can be found in a two atom configuration. For the purpose of clarity it is evaluated in the condensable category. It has a similar atomic mass and first ionization energy to xenon, and consequently is cursorily capable of offering similar performance. Iodine is also a more abundant resource, therefore having a fraction of the cost of xenon.

The physical and ionization properties of iodine are summarized in Table 1. At normal temperature and pressure iodine is a high density solid (3 times the pressurized density of xenon) which can sublimate substantially. With a decrease in pressure and increase in temperature, iodine can achieve high vapor pressure up to 23 kPa at the melting point (113.7 °C — Fig. 5). Therefore only moderate heating of 5–10 W is required to raise the temperature of the propellant to sustain sufficient flow rates. The uniquely high vapor pressure resulting from a low thermal input allows iodine to also be used in other thruster types such as cold gas thrusters [77]. The solid storage of iodine presents advantages over xenon as no pressure vessels are required, reducing system complexity and allowing for the storage tank shape to vary such that it can integrate more easily inside the spacecraft volume. The ionization potential for molecular and atomic iodine (9.4 eV and 10.5 eV respectively) is significantly lower than that of xenon (12.1 eV). In addition iodine's dissociation energy is only 1.54 eV, and consequently the process of combined dissociation and first ionization of a single iodine atom will occur from an energy input of 11.99 eV, which closely matches the ionization energy of xenon [100]. At higher energies the process of dissociation and first ionization of both iodine atoms occurs at an energy of 22.5 eV, which is lower than the energy required to produce two xenon ions [100].

Plume diagnostics of a 200 W iodine fed Hall thruster have indicated that dissociation is dominant, with $I+$ species accounting for > 95% of the exhaust plume by mole fraction [25]. However, given that the energetic effects of dissociation are minimal, iodine thrusters have been shown to offer close to identical performance to those using xenon [101]. Examination of the exhaust plume of iodine thrusters has also shown that a more collimated beam can be produced with iodine, particularly at higher powers, contributing to its good performance [103].

Iodine is a member of the halogen group of elements, and as a result it is reactive. This impacts both the inner surfaces in contact with iodine propellant as well as potentially the surface of the spacecraft. Research shows that refractory metal behavior is favorable in

a saturated iodine vapor although localized pitting in long exposure times is present [63]. Other metallic substances and polymers have shown accelerated corrosion with more detrimental behavior in lighter transition metals [63]. The long term impact of iodine on testing and spacecraft surfaces was identified at an early stage of development as one of the primary barriers to the adoption of iodine [68,100]. In order to test safely iodine-based systems specialized equipment is required, such as refrigerated exhaust collection panels [102,108]. Plume shields have also been tested to determine if a simple barrier can be used in test facilities to prevent the degradation of surfaces [103]. These experiments have shown that surface coatings, such as nickel plating, provide the greatest protection to test surfaces, while simple plume shields were ineffective. Vacuum chamber effects and reflection may amplify reaction rates between the propellant and spacecraft surfaces as seen with metallic propellant reflective deposition [67].

A secondary system wide concern is propellant surface deposition. Thermal control of spacecraft surfaces has been suggested as a method of preventing deposition [68,103]. This method was demonstrated on the SERT-II mission, which collected mercury deposition rates via the surface contamination experiment [87]. The majority of surfaces showed no signs of mercury condensate [87]. Examination of the deposition rate versus the evaporation rate of iodine was performed by Szabo et al. [103], and showed that for a 1 kW thruster there was no accumulation of iodine above −75 °C.

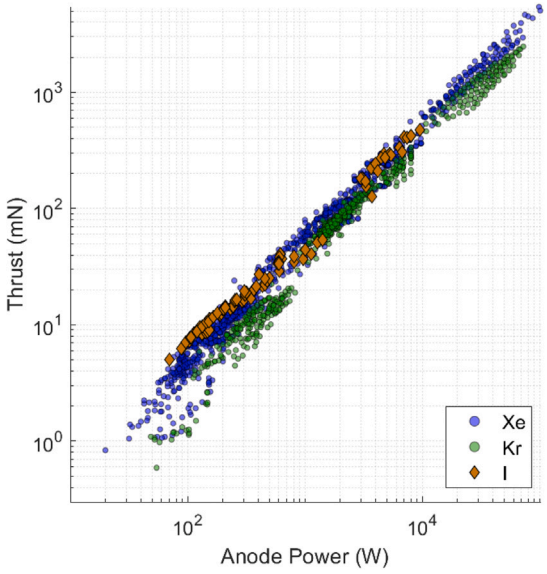

Fig. 15. Thrust vs anode power for Hall thruster operating on iodine.

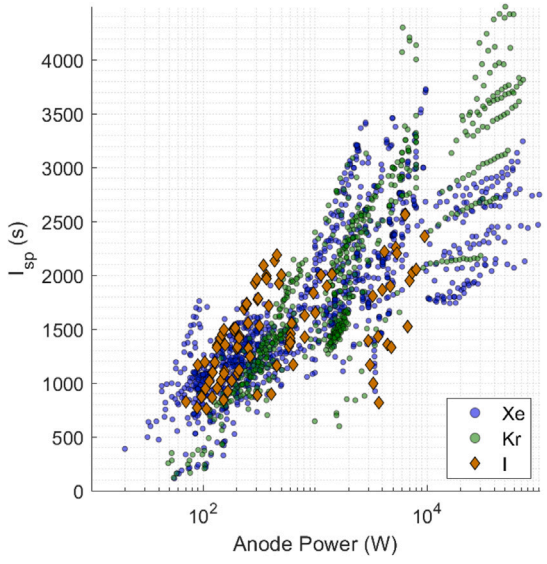

Fig. 16. Specific impulse vs anode power for Hall thruster operating on iodine.

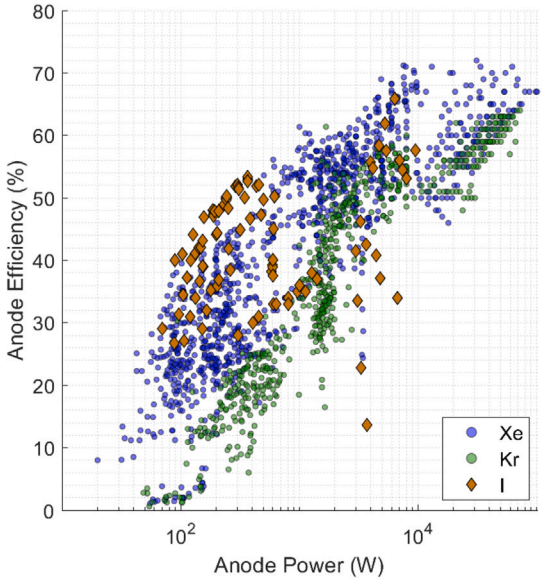

Fig. 17. Efficiency vs anode power for Hall thruster operating on iodine.

Propellant feed systems are also an area of active research for iodine-fed Hall thrusters. Several difficulties are faced by these systems, such as thermal management and heating of feed pipework, material compatibility and corrosion prevention, and flow control. Iodine is a brittle material that does not adhere well to heating surfaces with superficial mechanical processing of the element. Instead, it must be melted and cast on or within the heating system to achieve efficient packing and heat conduction. Iodine only requires modest heating (up to an approximate working temperature of 80–100 °C — approximately 5 W of power is required) in order to substantially sublimate and produce a high vapor pressure of more than 2 kPa. Due to the condensable nature of the propellant, the wetted area within the propellant feed and transport system must also be maintained above the melting temperature to prevent clogging and deposition [64]. The parasitic power requirements for the propellant and feed heating system are low in the order of up to 5–10 W, one of the lowest in all condensable propellants. The high vapor pressure of iodine resembles that of a pressurized gaseous propellant requiring the flow to be restricted to the desired rate. Flow control has been demonstrated with a standard flow controller [109] as well as with a temperature controlled area constriction [51].

A comparison between xenon, krypton and iodine is shown in Figs. 15 16 17. Iodine performance is excellent in Hall thrusters in particular below 1 kW. Experimental data on the Busek BHT-200 demonstrates high efficiency with iodine as a propellant peaking at 53% anode efficiency at 367 W discharge power [25]. A specific impulse of 2010 s was also demonstrated at 500 W discharge. Iodine was also used in high power thrusters, specifically the BHT-8000 demonstrating operation up to 9.5 kW. The highest anode efficiency recorded was 65% at 2.5 kW discharge power [103].

3.7. Ionization characteristics

The ionization energy is used to estimate the difficulty involved in ionizing the propellants identified as potential alternatives to xenon.

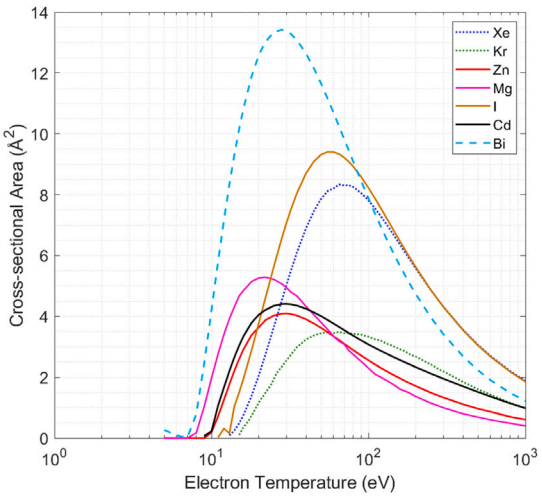

Fig. 18. Electron impact ionization cross-sectional area versus electron temperature for a selection of Hall thruster alternative propellants. Data from: Xe, Kr [110]; Zn, Mg, I, Cd [111]; Bi [112].

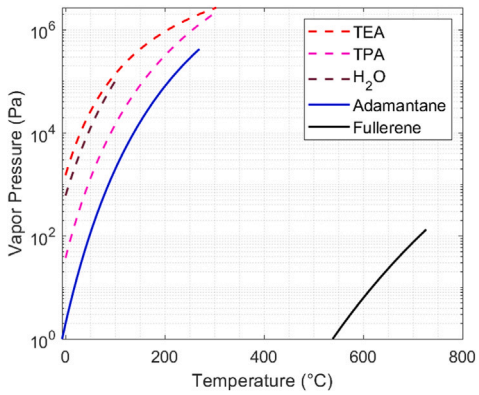

Fig. 19. Vapor pressure versus temperature for a selection of tested Hall thruster molecular propellants. Propellant phase: solid — solid line; liquid — dashed line; Equations from [113–117].

Assuming ionization through electron impact, the relationship between cross-sectional area and electron temperature is drawn in Fig. 18.

Any energy that is used to ionize the propellant is not available to be used to generate thrust, therefore elements with lower ionization energies are capable of more efficient operation. The lowest ionization energy is exhibited by bismuth, magnesium, cadmium and zinc followed by iodine and xenon. The largest ionization cross-sections are found in bismuth, magnesium, iodine and zinc followed by xenon and krypton.

Amongst the propellants bismuth and iodine distinguish as having a higher ionization efficiency than xenon and the other propellants. Zinc and magnesium however require a lower ionization energy than xenon. In a Hall thruster that is designed to maximize the propellant residence time within the discharge chamber, the detrimental effect of the cross-sectional area on the probability of impact ionization of zinc and magnesium is reduced. Overall, ionization characteristics of condensable propellants are more favorable than those of krypton, the closest competitor to xenon.

4. Molecular propellants

A third class of potential xenon propellant alternatives in Hall thrusters are molecular propellants. Molecular propellants can offer a theoretically wide performance band through their highly variable atomic composition and their respective added mass. The mass of a molecule can be orders of magnitude greater than the heaviest element, potentially of interest to applications that require very high thrust-to-power ratios. Equally, molecular propellants can have a mass similar to xenon replicating theoretically the performance of the gas. The number of potential molecular propellants that could be investigated is very wide, with tailoring of the molecule possible to achieve the ideal performance for a particular mission. Amongst the currently investigated propellants we find adamantane, triethylamine (TEA), tripropylamine (TPA), fullerene, water, oxygen, carbon dioxide, and nitrogen.

4.1. Vapor pressure, fragmentation and toxicity

Similar to condensable propellants, some molecular propellants require heating to sublimate or evaporate their gas phase for ionization. As a result, an additional power penalty is expected. TEA, TPA and water are liquid at normal temperature and pressure while fullerene and adamantane are solid. TEA, TPA and water are volatile and can achieve a high vapor pressure without significant heat addition [113–115] and consequentially a high operational vapor pressure of more than 10^4 Pa. Adamantane is found in solid state at normal conditions and produces vapor through sublimation with little heating [116]. Adamantane, TEA, TPA and water behave similarly to iodine by producing a high vapor pressure at low temperature inputs. Therefore, their gas phase flow rate must be restricted to ensure flow control. Fullerene is a solid and behaves similarly to bismuth due to the much heavier mass. Substantial sublimation occurs past 600 °C and does not drastically increase with temperature peaking roughly at 133 Pa close to 720 °C. Notably, fullerene sublimation is highly dependent on purity and thus experimental data show consistent variation in recorded output [117,118]. Similar to condensable propellants, additional power is required to maintain the feed system hot enough to prevent condensation along the propellant transport path for adamantane and fullerene as well as for TEA, TPA and water. Vapor pressure curves for the presented molecular propellants are shown in Fig. 19.

Other molecular propellants such as oxygen and carbon dioxide are found in gaseous form and can be utilized in a conventional xenon propellant storage and delivery system.

Ionizing a molecular propellant without dissociation is a major difficulty and represents the main challenge in high performance operation. The energy required for the first ionization of a molecule is typically higher than the bond energies between the molecule constituents. Molecular dissociation (fragmentation) will therefore occur, reducing the thrust produced as energy is lost in vibrational and rotational modes [119]. The exact make up of the fragmented molecules produced may also be difficult to know a priori.

Typical bond dissociation energies are in the range of 3–5 eV for symmetric dissociation and 10–13 eV for asymmetric dissociation. In comparison, typical first ionization energies range from 7–17 eV for molecular compounds. It should also be highlighted that the peak cross section of ionization for most substances occurs at 70 eV. The vast majority of ions created by electron impact are vibrationally excited well above their dissociation energies, resulting in significant molecular fragmentation.

In terms of toxicity, water is considered to have the lowest risk. Oxygen and carbon dioxide can act as toxicants only in high concentrations. Other molecular propellants such as adamantane ($C_{10}H_{16}$) and fullerene (C_{60}) are considered to also have low toxicity. However, degradation of the molecules may cause increased carcinogenic risk upon ingestion [120]. Triethylamine (TEA) and tripropylamine (TPA) are considered to be toxic, and may be corrosive and inflammable under certain conditions making them hazardous substances.

4.2. Adamantane ($C_{10}H_{16}$)

Several studies have investigated molecular propellants for use within various different electric propulsion systems. Diamondoids are a group of materials with some properties that make them favorable for use as a propellant. The lightest of the group, adamantane ($C_{10}H_{16}$), has a mass of 136.24 u, which is similar to that of xenon. It also has a lower first ionization potential at 9.23 eV [121], has low production costs, and can be brought into gas phase with only moderate heating. In solid form the density of adamantane is 1.08 g/cm^3 which is higher than that of unpressurized xenon. Fragments of adamantane are expected when electrons above 10.6 eV are present in the plasma [119]. Analysis of the exhaust plume of a gridded ion thruster operating with pure adamantane showed significant fragmentation to be occurring [122]. Hall thruster ignition and operation with adamantane was also demonstrated [123] with both thruster and cathode fueled by sublimated adamantane. Post experiment inspection of the cathode system showed significant carbon deposition within the system.

4.3. Tripropylamine (TPA) ($C_9H_{21}N$) and triethylamine (TEA) ($C_6H_{15}N$)

Recent studies have investigated tertiary amines as a propellant in cylindrical Hall thrusters [26]. Triethylamine (TEA) $C_6H_{15}N$ with a mass of 101.2 u and tripropylamine (TPA) $C_9H_{21}N$ with a mass of 143.3 u have been identified as possible propellants. Both propellants have a lower first ionization energy of 7.53 (TEA) and 7.40 (TPA) compared to xenon at 12.127 eV. A low power cylindrical Hall thruster was operated with TEA and TPA successfully [26]. Good performance was achieved, with efficiencies approximately 20% less than the xenon operation benchmark on the same thruster. There was firm spectroscopic evidence of molecular fragmentation occurring within the thruster and plume, with this being identified as the main cause of lower performance in comparison to xenon operation. Significant carbon deposits were also identified within the discharge channel of the thruster [26].

4.4. Fullerene (C_{60})

Buckminsterfullerene (fullerene C_{60}) has also been investigated for use as a propellant for ion propulsion systems [124–126]. C_{60} possesses a very high mass of 720.66 u, over five times that of xenon, as well as a low first energy of ionization (7.61 eV) [127] and an extremely large ionization cross section (25 $\forall^2$) [128]. In order to phase transition the C_{60} to a gas, high temperatures are required due to a natural low vapor pressure [117]. Reports suggest significant thermal fragmentation of C_{60} molecules at temperatures exceeding 800°C and total fragmentation at temperatures of 1000°C [126]. Operational temperatures for C_{60} vaporization are above 600–700 °C, close to the thermal fragmentation threshold. As a result it is difficult to produce C_{60} in gaseous form without the thermal energy input dissociating the molecule. Molecular fragmentation during ionization is also expected to still greatly affect the performance. Finally, the price of high purity C_{60} is high comparable to that of xenon making C_{60} only attractive in specific high thrust scenarios due to the large mass of the molecule. Hall thruster operation on fullerene was demonstrated with relatively low efficiencies [129]. The observed performance degraded over time in correlation with increasing heavy carbon deposition on the thruster surface and discharge chamber. As fragmentation of C_{60} is likely to occur above the 750–800 °C temperature threshold, anode/propellant distributor temperatures may contribute to degradation through fragmentation of the propellant before ionization occurs. Secondly, processes of electron–ion recombination, recycling of ions into neutral particles at solid surfaces, charge exchange between ions and neutrals, and electron attachment to carbon species may further contribute to carbon buildup on the thruster and channel surfaces [129].

4.5. Water (H_2O)

The current research effort focuses on the use of water (H_2O) as a propellant in Hall thrusters [130–132]. The advantages of water are the low cost and low toxicity coupled with wide availability in the Solar System, unlocking the potential of in-situ propellant acquisition and utilization [133]. Water is a light propellant with an atomic mass of 18.02 u, implying a theoretically high specific impulse achievable in Hall thruster operation [131]. The first ionization energy of water is 12.65 eV which is close to xenon (12.1 eV) [134,135]. The total ionization cross sectional area of a water molecule (2.32 $\forall^2$ [134]) however is smaller than that of xenon (5 $\forall^2$) leading to increased ionization difficulty. Water can be stored in liquid state at higher densities than krypton or argon yet at lower densities than other propellants such as iodine or zinc amongst others. Another advantage of water is the ability to electrolyze the propellant for hydrogen and oxygen extraction enabling usage of chemical propulsion systems or a multi-mode electrical–chemical propulsion system [131,136]. Cathode integration is further simplified since extracted hydrogen may be used as the cathode propellant [137]. Studies on water usage in hall thrusters have shown a relatively low efficiency in the order of 4–13% [130,132] which can be attributed to dissociation as well as plasma instability. Thruster design parameters have been shown to contribute significantly to the theoretical performance of water as a propellant [138].

4.6. Oxygen (O_2), carbon dioxide (CO_2) and nitrogen (N_2)

There has been various investigations into the use of other molecular gases within Hall thrusters, in particular within the scope of air breathing electric propulsion [48,139]. The propellants proposed are oxygen (O_2), carbon dioxide (CO_2) and nitrogen (N_2) as they can be found in various percentages within planetary atmospheres in the solar system. They have wide availability and low price and can be regarded as non-toxic. The propellants can be used independently or in a mixture replicating the planetary atmosphere conditions at a certain altitude or within a different planetary atmosphere.

Carbon dioxide is the heaviest of the three molecules at 44.01 u, oxygen the second at 32 u and nitrogen the lightest at 28.02 u [140]. Given the lower mass of the molecules compared to xenon, the molecules have faster thermal velocities, and so a shorter residence time within the discharge channel. The first ionization energies of the three molecular propellants are 13.78 eV for CO_2, 12.07 eV for O_2, and 15.58 eV for N_2 [140,141], all higher than the first ionization energy of xenon (12.1 eV) with the exception of O_2. Coupled with a smaller total ionization cross sectional area than xenon at 2.5 $\forall^2$ N_2, 2.8 $\forall^2$ O_2 and 3.5 $\forall^2$ CO_2 [141,142], difficulty in ionization is expected with a reduced probability of electron impact. Thruster channel lengths become important design parameters to increase the ionization rate for these propellants [142]. Studies on Hall thrusters operating on pure N_2, O_2 and CO_2 are limited [131,142,143] showing poorer efficiency peaking in the range of 22%–28% anode efficiency compared to operation on gas mixtures.

Recent studies demonstrate the ignition of the thruster on nitrogen–oxygen mixtures, with thrust achieved at the mN level [47,144]. Work has also been completed investigating Hall thrusters using CO_2 mixtures for operation in the Martian atmosphere [48,145]. Hall thrusters operating on mixtures of Xe with N_2 and air have also been demonstrated [146]. The current research focus is on the development of air breathing concepts for very low altitude orbits, of approximately 200 km. Efficiencies as high as 27% have been achieved on atmospheric air compositions representing altitude of 150 km in Hall thrusters at 2–2.5 kW [48]. Similarly, Hall thrusters operating on martian atmosphere composition of predominantly CO_2 achieved an overall efficiency in the range of 20%–25% with thrust to power ratios of 30 mN/kW [48].

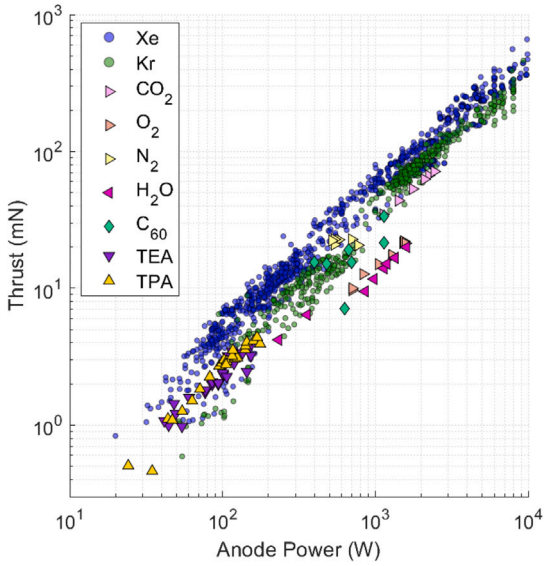

Fig. 20. Thrust vs anode power for Hall thruster operating on molecular propellants.

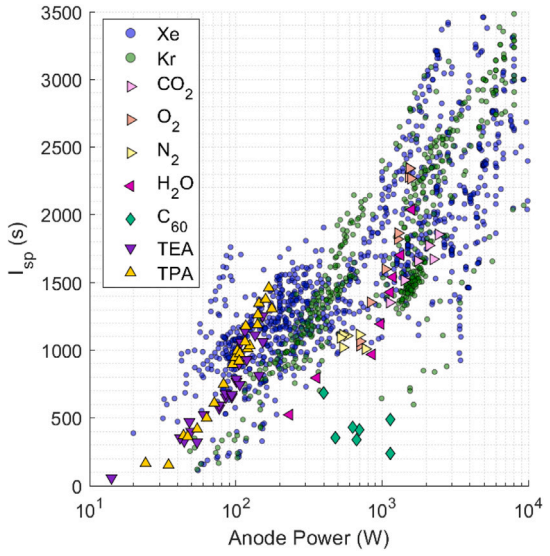

Fig. 21. Specific impulse vs anode power for Hall thruster operating on molecular propellants.

4.7. Performance overview

As with most alternative propellants discussed in this study a limited data set is available for molecular propellants in standard configuration Hall thrusters. Data on Hall thruster performance on molecular propellants is shown in Figs. 20, 21, and 22 showcasing thrust, specific impulse and efficiency for a wide selection of thrusters as well as xenon and krypton.

In the low power range below 200 W, TEA and TPA show good performance with higher thrust, efficiency and specific impulse compared to available krypton data. TEA and TPA are very closely matched in terms of thrust, specific impulse and efficiency with TPA showing slightly better performance peaking at approximately 18.5% anode efficiency (TPA). The maximum thrust was approximately 4.3 mN (TPA) and peak specific impulse 1460 s (TPA) [26]. With controlled usage to mitigate toxicity risks, TPA and TEA are highlighted as being promising propellant alternatives to xenon.

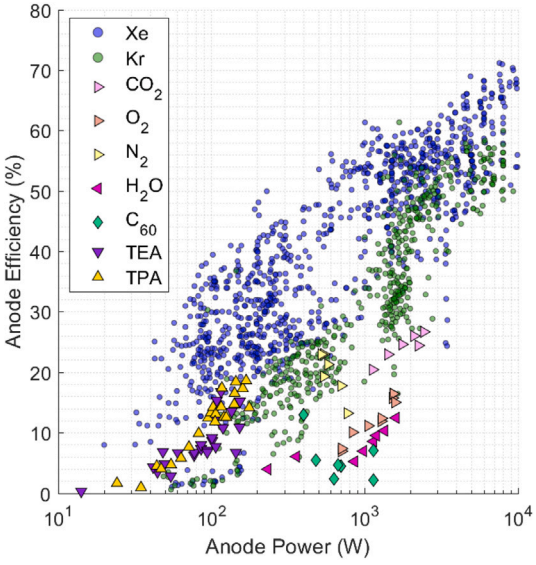

Fig. 22. Efficiency vs anode power for Hall thruster operating on molecular propellants.

Up to 1 kW, nitrogen has the highest performance with a maximum anode efficiency of 23% in the available dataset [142]. At this point the thrust generated is 22.76 mN with a specific impulse of 1114.16 s.

In the upper power bracket above 1 kW, the performance of molecular propellants is reduced with krypton performing significantly better. Yet notably, oxygen and carbon dioxide can achieve a high specific impulse in the range of 1700–2300 s at 1.5–2 kW [48,130] albeit at an efficiency penalty, peaking at 26% for carbon dioxide. Fullerene is also a good candidate for high thrust scenarios achieving a maximum thrust of 33.6 mN [129] yet displaying significant losses due to fragmentation and other recombination mechanisms. With the added power requirements for the propellant phase change, fullerene performs poorly in the overall assessment compared to other molecular alternatives. Finally water as a propellant succeeds in achieving a high specific impulse yet thrust and overall efficiency are low. However, these drawbacks are offset by the possibility of in-situ propellant utilization along with the ability to operate chemical thrusters from hydrogen and oxygen extracted through electrolysis.

The study of alternative molecular propellants is still ongoing with significant progress being made in the development of a cheaper and readily available replacement propellant to xenon.

5. Hollow cathode considerations

A hollow cathode is a critical component within Hall thruster systems, serving to sustain the ionization process, and neutralize the plume. The cathode is only briefly discussed in this study in the context of alternative propellant operation.

A typical hollow cathodes consists of a low work function emissive material that releases electrons through thermionic emission. To avoid space charge limitations a gas is fed into the hollow cathode, with typically the same propellant used for the cathode as for the thruster itself. Therefore, the issue of compatibility between the propellant and the emissive material is a large concern for the selection of alternative propellants.

Barium oxide (BaO) impregnated tungsten is perhaps the most commonly used cathode emissive material with EP systems. Low energy electrons are produced by heating a barium-on-oxide mono-layer that forms on the surface of the tungsten matrix. As the barium and barium oxide is continuously evaporated from the emitter surface, BaO cathodes rely on two processes to replenish the surface layer: a chemical

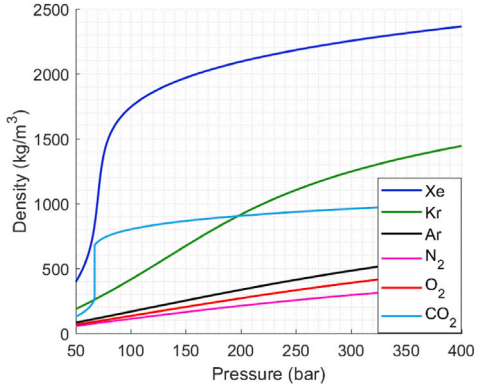

Fig. 23. Density vs pressure for different gaseous propellant options at a temperature of 300 K. Data from the NIST database.

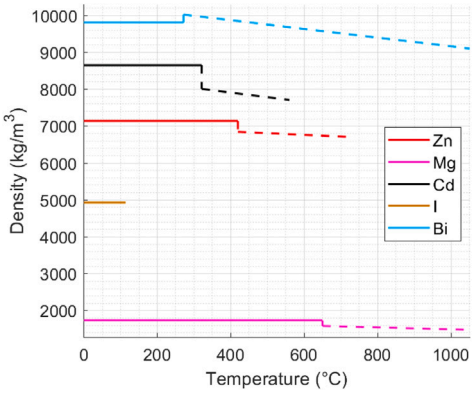

Fig. 24. Density vs temperature for different condensable propellant options: solid — solid line; liquid — dashed line; Data from [157–160].

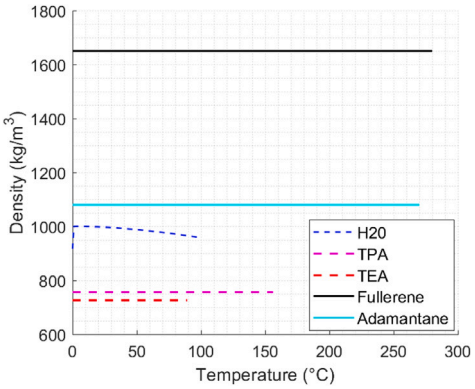

Fig. 25. Density vs temperature for different molecular propellant options: solid — solid line; liquid — dashed line; Data from Merck.

reaction with the tungsten matrix to produce the barium, and diffusion through the matrix that brings the barium to the surface [147]. This reliance on chemical processes makes BaO cathodes susceptible to poisoning as electronegative gases such as oxygen can be chemically adsorbed into the emitter, altering the processes and increasing the material work function. Operation of BaO hollow cathodes has been demonstrated noble gases, and also operation using iodine although not including long term testing [147].

Lanthanum hexaboride (LaB_6) is another popular emitter material that possesses significant flight heritage [24]. LaB_6 cathodes are less sensitive to poisoning than those that use BaO, as there is no reliance on chemical processes since the entire bulk is emissive. LaB_6 cathodes have been demonstrated successfully with a range of propellants, including the noble gases but also more reactive elements such as hydrogen, oxygen, and bismuth [148–150]. LaB_6 has also been used as the emissive material within a hollow cathode operating on lithium [151], designed for use with a very high I_{sp} gridded ion thruster [152].

There are currently various other materials under consideration for use as the insert of an alternative propellant hollow cathode, in particular for use with iodine [153,154]. One novel insert material is calcium aluminate electride, $C_{12}A_7$. As well as having a very low work function, it has been reported to be iodine compatible, although with operation for only 20 hours [155]. Propellant compatibility with cathode materials is not only limited to the emissive insert. Highly reactive propellants such as iodine are known to negatively interact with steel and tungsten, both of which are commonly used materials in cathode design [156].

To summarize, hollow cathodes with a high degree of compatibility is an ongoing area of research, and although initial results look promising with regard to operation with harder to handle alternative propellants, further research is required.

6. Propellant density

The density of an element is also of significant importance to its selection as a propellant. A higher density allows for a greater quantity of propellant to be stored in a smaller volume. Xenon is the most dense of the noble gases at 1600 kg/m^3 when stored above 80 bar followed by krypton and argon as shown in Fig. 23. Unlike xenon, krypton requires a much higher storage pressure to increase the density making it less volume efficient. The high pressure vessels required to maintain higher densities can place limitations on the available space for other spacecraft systems.

Condensable propellants are naturally much more dense than gaseous elements, as shown in Fig. 24. Their solid state densities range from as low as 1738 kg/m^3 in the case of magnesium (slightly higher than the density of pressurized xenon), to as high as 9747 kg/m^3 in the case of bismuth. However, the density of the propellant registers a significant drop past the melting point highlighting an important design consideration. Notably a liquid phase change of bismuth has the opposite effect of increasing its density by a small margin exceeding 10,000 kg/m^3.

Molecular propellants densities range from 726 kg/m^3 TEA and 756 kg/m^3 TPA in liquid state to 1080 kg/m^3 adamantane and 1650 kg/m^3 fullerene in solid state with water at approximately 1000 kg/m^3. A comparison of liquid/solid molecular propellants is shown in Fig. 25. These values are lower than pressurized gaseous alternatives indicating a larger volume penalty for propellant storage.

7. Financial cost

To provide a complete overview of propellant options, a cost comparison of selected propellants is presented. The USD price per kilogram or liter is shown in Table 2.

The purity of the element is a major factor that influences the overall cost. Where possible, the highest purity of above 99.99% was used in the cost table. However, in real world applications lower purities may be sufficient, as a result the propellant will be at a much lower cost. Given the fluctuating nature of the market where prices may increase or decrease in response to external factors, the values presented in Table 2 are intended as a guideline in propellant cost ranking.

Condensable propellants such as zinc, cadmium, magnesium and bismuth are the cheapest in the current market, with iodine a more expensive alternative yet much cheaper than xenon.

Table 2
Price evolution for selected elements. +Price derived from flask data; * according to U.S. Geological Survey 2022 [98] ** according to Merck ; *** Various independent suppliers;.

Purity 99.99%	Market	2017	2018	2019	2020	2021	2022
USD/l							
Xe**	European Market	–	–	–	–	910.97	1,050.00
Kr**	European Market	–	–	–	–	177.86	204.00
Ar**	European Market	–	–	–	–	218.91	243.00
O_2^{**}	European Market	–	–	–	–	169.88	195.00
N_2^{**}	European Market	–	–	–	–	169.88	195.00
CO_2^{**}	European Market	–	–	–	–	182.42	195.00
USD/kg							
Zn*	North American	3.07	3.11	2.74	2.44	3.20	–
	London Metal Exchange	2.89	2.93	2.55	2.26	3.00	–
Cd*	North American	1.75	2.89	2.67	2.29	2.49	–
Mg*	U.S. Spot Western	4.74	4.78	5.40	5.49	8.60	–
	European Free Market	2.27	2.55	2.43	2.15	5.50	–
Bi*	North American	10.89	10.16	7.01	6.00	8.05	–
I_2^*	North American	19.55	22.46	26.38	31.57	32.00	–
Cs*+	North American London Metal Exchange	–	–	–	65200.00	69900.00	–
Hg*	European Union	30.20	31.91	–	–	–	–
	Global	36.93	78.59	73.98	–	–	–
USD/kg							
*TEA***		–	–	–	–	150.47	398.07
*TPA***		–	–	–	–	66.00	113.70
*Adamantane****		–	–	–	–	540.00	721.36
*Fullerene****		–	–	–	–	493.30	1,000.00

Molecular propellants are more expensive than their condensable counterparts with a drastic increase above 99.9% purity for larger quantities.

Finally rare gasses are the most expensive at high purity with xenon at the top. In spite of this, xenon still remains the standard propellant in EP albeit at a non-negligible percentage of the total cost of the spacecraft.

8. Mission scenario study

To conclude the theoretical review of propellants, an analysis of propellant performance in Hall thrusters is proposed based on a set of potential mission parameters. The scenarios presented range from low power, small spacecraft station keeping needs to high power interplanetary travel. The viability of a subset of propellants is explored in the specified power bracket and their drawbacks highlighted. For brevity, argon, nitrogen, oxygen, carbon dioxide and water are not included in this calculation due to the relatively low experimental performance exhibited. For consistency, the power brackets are defined as follows: low power — ≤1 kW; medium power — 1 kW–2.5 kW; high power — ≥2.5 kW.

The input parameters for the calculations presented are simplified to thruster power, thruster discharge voltage, spacecraft dry mass and required total delta v (Δv). Ideal thrust and specific impulse calculations are performed based on propellant mass (M in kg) and thruster power ($P = I_b V_b$) according to the following equations [37]:

$$I_{sp} = \frac{1}{g_0}\sqrt{\frac{2eV_b}{M}}, \tag{10}$$

$$T = \sqrt{\frac{2M}{e}} I_b \sqrt{V_b}, \tag{11}$$

where e represents the elementary charge and g_0 gravitational acceleration. Efficiency terms are not included in this calculation since they depend on propellant performance within a specific thruster and can range significantly depending on thruster design. The propellant mass is then extracted from the Δv equation using the previously calculated ideal thruster performance and the input spacecraft dry mass:

$$\Delta v = (g_0 I_{sp}) log\left(\frac{m_d + m_p}{m_d}\right). \tag{12}$$

Finally, the propellant flow rate $\dot{m}_p$ is extracted from the specific impulse–thrust equation:

$$I_{sp} = \frac{T}{\dot{m}_p g_0}. \tag{13}$$

To produce a fair comparison, a minimum power calculation is conducted for condensable and molecular propellants according to the theoretical background presented in Section 2.2. In this case, an external tank design coupled with a gas distributor anode is assumed (Fig. 11). Consequently, propellant transport is also included in the calculation for a better power estimation. Eqs. (1), (2), (6) and (9) are combined and solved numerically. To generate an exposed area, the propellant bulk is assumed to be a cube with a volume given by the required propellant mass and the specific propellant density. Finally, the diameter of the feed is assumed to not exceed the height of the Hall thruster discharge channel since the most common method of propellant distribution is through the thruster anode. This assumption relates the propellant transport requirements to the size of the thruster. As a result, an estimation of the thruster size is required to finalize the calculation. This is achieved through a set of scaling laws that are used in the preliminary design of Hall thrusters [161]. For comparison xenon and krypton are included in the propellant estimation and are assumed to be pressurized at 200 bar respectively.

8.0.1. Station keeping scenario

The first theoretical scenario simulates the station keeping requirements of a small $m_d = 50$ kg spacecraft that requires a total of $\Delta v = 1$

Table 3
Scenario 1 — Station keeping of a small spacecraft propellant performance comparison (100 W Hall thruster). Cost estimated on 2021 market data.

Power Rating (W)	**100**
Voltage (V)	**100**
Delta V (m/s)	**1000**
Dry Mass (kg)	**50**

	Xe	Kr	I	Mg	Zn	Bi	Cd	TPA	TEA	$C_{10}H_{16}$	C_{60}
Burn Time (h)	877.60	1089.32	892.02	1991.89	1228.46	703.27	945.49	841.69	994.57	862.19	396.42
Propellant Mass (kg)	4.30	3.41	4.22	1.81	3.00	5.48	3.97	4.50	3.76	4.38	10.66
Propellant Volume (l)	2.06	3.76	0.86	1.04	0.42	0.56	0.46	5.98	5.17	4.06	6.46
Flow Rate (mg/s)	1.36	0.87	1.32	0.25	0.68	2.17	1.17	1.48	1.05	1.41	7.47
Ideal Isp (s)	1236.24	1547.41	1257.43	2873.26	1751.86	979.87	1336.04	1183.44	1408.17	1213.59	527.66
Ideal Thrust (mN)	16.50	13.18	16.22	7.10	11.64	20.81	15.26	17.23	14.48	16.80	38.65
Total Impulse (kNs)	52.12	51.68	52.08	50.90	51.48	52.69	51.96	52.22	51.85	52.16	55.16
Tank Power (W)	-	-	<5	37.97	12.30	206.91	7.26	<5	<5	<5	220.42
Propellant Cost (USD)	9884.58	3188.26	135.16	15.53	9.59	44.14	9.87	296.96	563.25	236.67	5258.24

Table 4
Scenario 1 — Station keeping of a small spacecraft propellant performance comparison (300 W Hall thruster). Cost estimated on 2021 market data.

Power Rating (W)	**300**
Voltage (V)	**200**
Delta V (m/s)	**1000**
Dry Mass (kg)	**50**

	Xe	Kr	I	Mg	Zn	Bi	Cd	TPA	TEA	$C_{10}H_{16}$	C_{60}
Burn Time (h)	408.68	508.53	415.48	934.09	574.15	326.44	440.70	391.74	463.85	401.41	181.52
Propellant Mass (kg)	3.00	2.38	2.95	1.27	2.10	3.82	2.77	3.14	2.63	3.06	7.32
Propellant Volume (l)	1.44	2.63	0.60	0.73	0.29	0.39	0.32	4.17	3.62	2.83	4.44
Flow Rate (mg/s)	2.04	1.30	1.97	0.38	1.02	3.25	1.75	2.23	1.57	2.12	11.20
Ideal Isp (s)	1748.30	2188.37	1778.28	4063.40	2477.51	1385.75	1889.44	1673.63	1991.45	1716.27	746.23
Ideal Thrust (mN)	35.00	27.96	34.41	15.06	24.70	44.15	32.38	36.56	30.72	35.65	81.99
Total Impulse (kNs)	51.49	51.18	51.46	50.63	51.04	51.89	51.37	51.55	51.30	51.52	53.58
Tank Power (W)	-	-	<5	26.95	8.72	161.18	5.12	<5	<5	<5	155.10
Propellant Cost (USD)	6904.55	2232.59	94.43	10.93	6.72	30.74	6.90	207.31	394.04	165.28	3611.57

km/s for a mission duration of 5 years. In this case, the size of the spacecraft limits the amount of available power for the propulsion system to 100 W. Assuming a discharge voltage of 100 V, the propellant performance is shown in Table 3.

In terms of performance at low power, xenon, iodine, TPA, TEA and adamantane ($C_{10}H_{16}$) show almost identical ideal specific impulse and thrust, and similar propellant flow rate requirements. The most drastic difference is the overall propellant volume. Iodine is the most advantageous due to its outstanding volumetric savings. Molecular propellants are less efficient due to lower density than pressurized xenon. Given that all of the highlighted alternative propellants produce high vapor pressure with minimal power input (<5 W), for this use case and power scenario, iodine is a strong alternative to xenon.

Other propellants such as bismuth and C_{60} are less desirable in the low power bracket since the total estimation of heater power exceeds drastically the thruster power. However, Hall thrusters operating on bismuth showed high anode efficiency towards the upper limit of the thruster power window closer to 1 kW showcasing the viability of this propellant when heating power costs can be included in the power budget of the mission. Magnesium and zinc highlight a potential compromise. Due to their high theoretical specific impulse, they require much less propellant for the same mission scenario than xenon or iodine albeit with the need for a longer burn time to achieve the same Δv. The heater power requirement is however more demanding at this scale. The heater power represents 38% of the total available power in the case of magnesium and 12% in the case of zinc. As a result zinc and magnesium are less desirable compared to iodine in this scenario.

If the available power is increased for the same spacecraft mass, a larger thruster may be used. Propellant performance data is shown in Table 4 for a 300 W thruster operated at 200 V in the same mission conditions (spacecraft mass m_d = 50 kg and a total Δv = 1 km/s). The coupled effect of higher thruster performance, lower total propellant mass, and less restrictive feed geometry as a result of larger thruster dimensions reduces significantly the required heater power for condesable propellants. In a 300 W thruster, magnesium heater power expenditure may be reduced up to 9% of the total thruster power available while zinc may draw approximately 3% of the total thruster power available. As a result zinc and magnesium become more competitive in terms of propellant mass, volume and cost compared to xenon. Iodine is still a power efficient, high performance, alternative to xenon while cadmium offers higher thrust and volume savings at a similar power input to iodine (5 W) at the cost of reduced specific impulse. Bismuth requires a higher propellant mass as well as a high fraction of the available power (53%) making its use unfeasible at this scale. Finally, TPA, TEA and adamantane ($C_{10}H_{16}$) can provide a similar performance to xenon yet they require a significantly large volume that might be detrimental at this scale.

An overview of experimental Hall thruster performance data within the low power range is shown in Fig. 26. The available experimental data set on alternative propellant usage agrees with the conclusions of the theoretical study. Iodine is a strong match to xenon performance while bismuth and zinc show good performance closer to the kW levels of power.

Overall the most promising propellant alternative to xenon in the low power thruster range (50 W–1 kW) is iodine. It offers considerable volume and cost savings while offering almost identical if not superior performance to xenon. The high achievable vapor pressure at a very low power input makes it suitable when available power is low. Finally, due to the inherent similarity to xenon, the Hall thruster design does not need to change to make efficient use of iodine as a propellant.

8.0.2. SMART-1 mission scenario

The second theoretical scenario simulates the SMART-1 mission profile where a SNECMA PPS-1350G Hall effect thruster was used [162, 163]. The thruster was operated between 462 W–1190 W [163]. An average discharge power of 1100 W is used for the propellant calculation. The discharge voltage for the operational thruster varies between 220 V and 350 V. The calculation assumes a set 300 V. The SMART-1 spacecraft has a m_d = 370 kg mass and required a total of Δv = 3.7 km/s. The theoretical propellant performance is shown in Table 5.

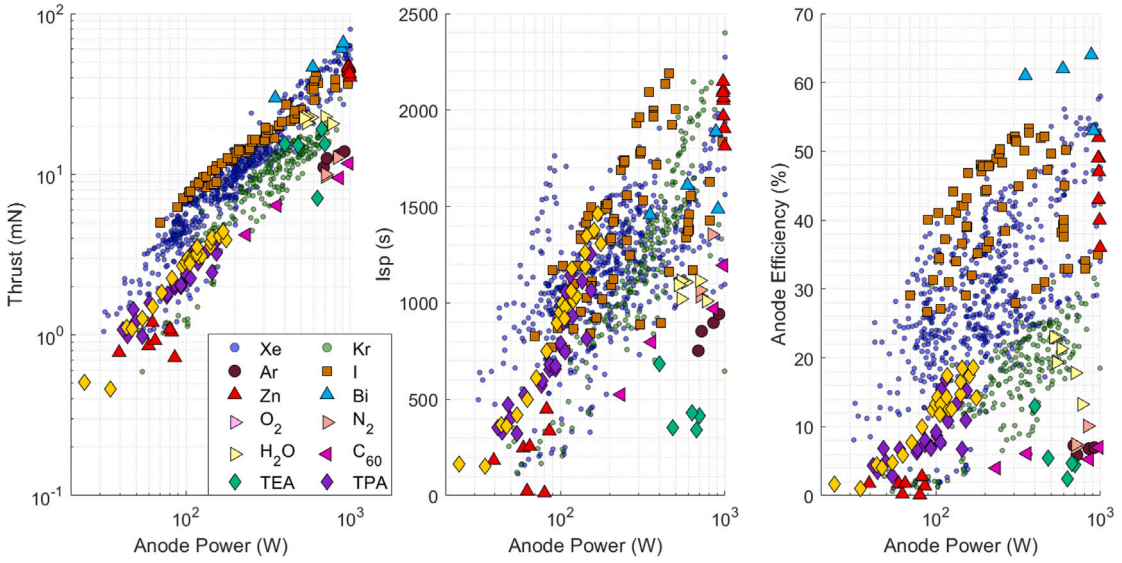

Fig. 26. Thrust, specific impulse and efficiency vs power for Hall thrusters operating on different propellants in the low power bracket up to 1 kW.

Total propellant mass calculations show that 71.29 kg of xenon would be needed for the duration of the mission. Flight data show that 81.72 kg of xenon were consumed in reality [163]. The result is a 13% difference in the estimation considering ideal thruster performance at a fixed power. Given the complexity of the thrust profile for the real mission and the subsequent variation in discharge voltage, power and propellant flow rate, the theoretical approximation is limited to showcase ideal performance at a set condition. With this limitations in mind, the data shown in Table 5 can still provide an insight into the behavior of alternative propellants in a medium power thruster in the context of a more complex mission scenario.

In this scenario, iodine can still provide a similar performance to xenon at a third of the price and half the propellant volume. Comparative experimental performance data shown in Fig. 27 highlights a slight drop in iodine efficiency, thrust and specific impulse. This may be due to a thruster size limitation. In the medium power thruster class, iodine still represents a good alternative propellant to xenon due to low cost, high density and modest heating requirements making it preferable over krypton.

Due to the large amount of propellant which the estimation assumes to be heated as a singular mass, power expenditure for bismuth exceeds the available thruster power. Consequently, heating up the whole mass of propellant would not be efficient. A solution to this issue could be bismuth propellant tank and management systems segmentation when scaling up towards higher power thrusters. A segmented design would involve multiple propellant tanks containing lower amounts of propellant (similar to Table 4 data) which can be managed with 150 W to 200 W of power. Upon depletion, a second tank can be heated and used to exhaustion and so on. This approach would make bismuth usage feasible in medium sized thrusters whist also providing a set of redundancies covering potential heater failure. A comparison between the theoretical performance of bismuth (Table 5) and experimental data points shown in Fig. 27 indicates very good agreement. In fact bismuth provides more thrust than xenon with a small specific impulse penalty at an overall high anode efficiency. Coupled with the excellent density of bismuth, the required propellant volume is reduced by approximately 3.6 times. The disadvantages of bismuth include higher propellant mass requirements for a similar Δv and the expensive heating power requirements. Nonetheless, bismuth may be successfully used in a mid power scenario predicting very good compatibility to high power thrusters.

Perhaps the most impressive propellant in the mid power scenarios is zinc. The bulk heating power cost of zinc is low at 63 W. A segmented design similar to the bismuth proposition can also be used to further lower the required vaporization power. The total zinc mass required is significantly reduced at approximately 68% of the total xenon mass required. Volume savings are further beneficial at 20% of the total xenon volume. Experimental performance data of zinc shown in Fig. 27 suggests that zinc may match the highest efficiency krypton thrusters and the lower efficiency xenon thrusters at approximately 45% anode efficiency in this power range in a xenon optimized thruster. Given the cost, mass and volume savings at a low heater power penalty, zinc is a strong alternative propellant for xenon in this bracket.

Magnesium presents similar benefits to zinc. Only 40% of the total xenon mass of propellant is required for the same mission while the volume savings are also high at 50% of the equivalent xenon volume.

Table 5
Scenario 2 — SMART-1 mission for a single 1.1 kW Hall thruster. Cost estimated on 2021 market data.

Power Rating (W)	**1100**
Voltage (V)	**300**
Delta V (m/s)	**3700**
Dry Mass (kg)	**370**

	Xe	Kr	I	Mg	Zn	Bi	Cd	TPA	TEA	$C_{10}H_{16}$	C_{60}
Burn Time (h)	3969.06	4878.59	4030.95	8764.02	5477.00	3221.80	4260.55	3814.95	4471.36	3902.94	1917.97
Propellant Mass (kg)	71.29	55.93	69.98	29.14	48.99	92.11	65.52	74.78	61.90	72.75	189.10
Propellant Volume (l)	34.08	61.76	14.20	16.75	6.86	9.39	7.57	99.30	85.26	67.36	114.60
Flow Rate (mg/s)	4.99	3.18	4.82	0.92	2.48	7.94	4.27	5.44	3.85	5.18	27.39
Ideal Isp (s)	2141.23	2680.20	2177.94	4976.63	3034.32	1697.19	2314.08	2049.77	2439.01	2101.99	913.94
Ideal Thrust (mN)	104.77	83.70	103.00	45.08	73.93	132.18	96.94	109.44	91.98	106.73	245.46
Total Impulse (kNs)	1497.02	1470.04	1494.73	1422.23	1457.75	1533.10	1486.92	1503.09	1480.56	1499.56	1694.83
Tank Power (W)	-	-	≈5	192.09	62.96	1338.13	37.17	≈5	≈5	≈5	1206.52
Propellant Cost (USD)	163915.69	52355.84	2239.47	250.62	156.77	741.50	163.15	4935.16	9284.98	3928.28	93281.57

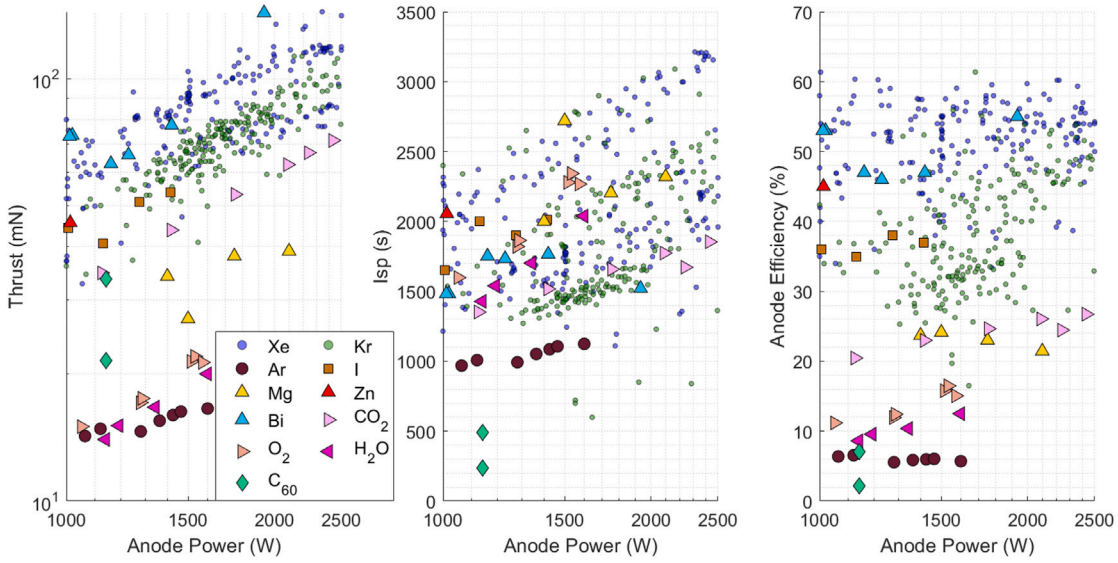

Fig. 27. Thrust, specific impulse and efficiency vs power for Hall thrusters operating on different propellants in the medium power bracket from 1 kW to 2.5 kW.

However, the propellant heater power cost is higher than zinc with the same possibility of propellant tank segmentation. Few experimental performance data points exist for magnesium however the available data set indicates a lower performance compared to zinc.

TPA, TEA and adamantane show similar theoretical performance to xenon. Their major drawback is the low density that leads to significantly larger propellant tanks. In this power bracket, the data available focuses on oxygen, carbon dioxide, water, and fullerene among other propellants. Given the scarcity of data, molecular propellants show good preliminary potential in the thrust and specific impulse with a relatively low anode efficiency which might be offset by in-situ propellant utilization.

Overall, the most efficient and promising propellant alternatives in the mid power thruster category are iodine, zinc, and bismuth with superior performance to krypton and even xenon at a fraction of the cost.

8.0.3. *Psyche mission scenario*

A final theoretical scenario simulates the Psyche mission profile where four SPT-140 Hall thrusters are used [164]. Since this larger scale mission utilizes a cluster of thrusters rather than a single unit, the propellant performance analysis addresses the total impulse requirements of a single thruster unit. Including safety margins and the requirement for a thruster redundancy in the cluster, a single thruster unit must sustain a total impulse of 5.5 MN-sec [164]. This translates into a total per thruster $\Delta v = 2.592$ km/s. The Psyche spacecraft mass is $m_d = 1648$ kg and the total propellant mass is 1030 kg. The SPT-140 can operate over a wide range of discharge power up to 5 kW [164,165] yet on the Psyche mission, the thrusters will operate between 1.7 kW and 4.5 kW [166]. The discharge voltage for the operational thruster is 300 V. The experimental evaluation of the SPT-140 was undertaken between 200 V and 400 V [165]. For this analysis, an average discharge power of 2.5 kW is assumed at an average voltage of 250 V. The resulting propellant performance is illustrated in Table 6.

Propellant mass estimations with xenon show a 16% difference to the actual propellant mass when four identical thrusters are considered. Technical data show that the SPT-140 operates at a peak 1900 s specific impulse at 5 kW and 400 V discharge [165] which is very different from the 1950 s estimation at 2.5 kW and 250 V. Therefore, the differences observed is a consequence of ideal thrust and specific impulse estimations. Yet an alternative propellant overview of ideal propellant performance in high power thrusters can still be drawn.

At this scale, maintaining the propellant at a high temperature to generate the gas phase and sustain the required propellant flow rate involves significant amounts of power most notably with bismuth and C_{60}. Therefore propellant tank segmentation is crucial in keeping the power requirements low. As multiple tanks reduce the volumetric benefit of propellants such as bismuth and worsen the penalty of low density propellants such as C_{60}, a system level optimization study can be undertaken to find the mission adequate number of tanks by balancing tank heater power consumption and total volume. Bismuth and C_{60} can provide high thrust unmatched by other alternative propellants at this scale and are most suitable in high power thrusters due to the subsequent higher power budget. However, C_{60} suffers heavily from fragmentation as shown in previous experimental studies [129]. This

Table 6
Scenario 3 — Psyche mission scenarios for 1 of the 4 thrusters operating at 250 V–2.5 kW (4.5 kW Hall thruster).

Power Rating (W)	**2500**
Voltage (V)	**250**
Delta V (m/s)	**2592**
Dry Mass (kg)	**1648**

	Xe	Kr	I	Mg	Zn	Bi	Cd	TPA	TEA	$C_{10}H_{16}$	C_{60}
Burn Time (h)	4862.85	6002.84	4940.45	10867.43	6752.44	3925.14	5228.31	4669.57	5492.54	4779.92	2281.15
Propellant Mass (kg)	239.17	188.44	234.87	98.95	165.38	307.28	220.17	250.62	208.21	243.95	615.84
Propellant Volume (l)	114.35	208.09	47.64	56.87	23.16	31.33	25.45	332.83	286.79	225.88	373.23
Flow Rate (mg/s)	13.66	8.72	13.21	2.53	6.80	21.75	11.70	14.91	10.53	14.18	74.99
Ideal Isp (s)	1950.75	2441.77	1984.20	4533.93	2764.39	1546.22	2108.23	1867.43	2222.05	1915.01	832.64
Ideal Thrust (mN)	261.36	208.81	256.96	112.45	184.44	329.74	241.84	273.03	229.45	266.24	612.34
Total Impulse (kNs)	4575.50	4512.33	4570.16	4399.48	4483.43	4659.44	4551.90	4589.67	4537.01	4581.42	5028.58
Tank Power (W)	-	-	≈5	401.94	131.34	2981.18	77.08	≈5	≈5	≈5	2467.41
Propellant Cost (USD)	549911.29	176399.31	7515.77	850.95	529.22	2473.64	548.22	16540.86	31230.89	13173.50	303792.15

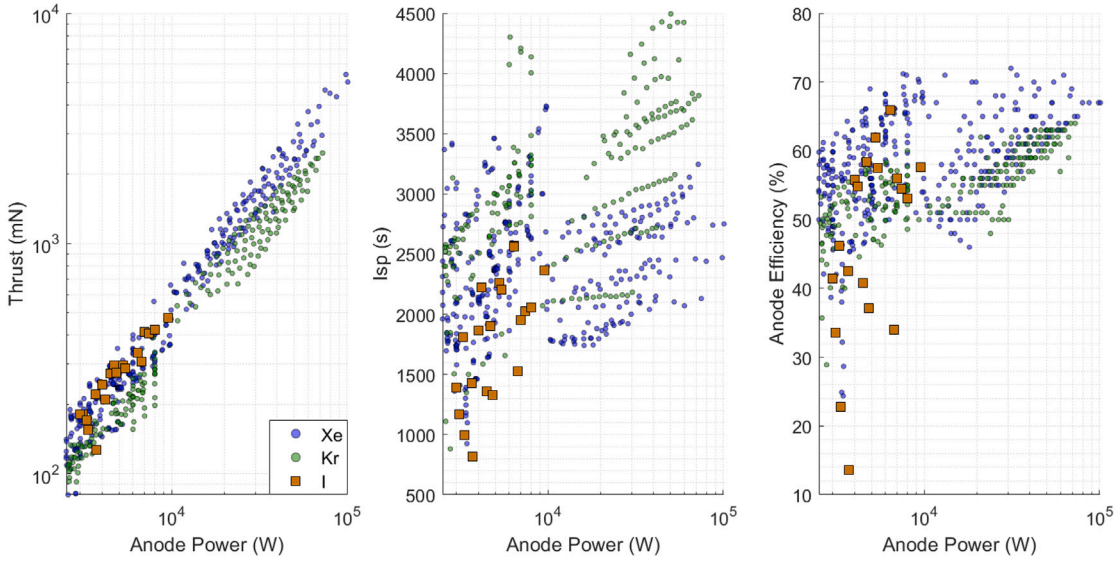

Fig. 28. Thrust, specific impulse and efficiency vs power for Hall thrusters operating on different propellants in the high power bracket above 2.5 kW.

makes bismuth the only viable choice at this high power level between the two propellants. Based on previous high power bismuth studies and mid range power experiments, bismuth is expected to be a very good propellant in this power bracket.

Zinc, iodine and magnesium are good alternatives to xenon in terms of price, volume and performance. Tank heater power peaks at 5% of the total available power to maintain the bulk of propellant at operational temperature in the case of zinc with much lower values for iodine. In this case reduced volume and propellant mass become more advantageous in spite of the increased power usage as approximately 300 kg of propellant can be saved with thrusters operating on zinc rather than xenon. However, the most promising propellant at this scale is magnesium. At the expense of higher heater power input requirements at 400 W per thruster (which can be reduced to 200 W or lower if the propellant is split in two or more tanks), the total propellant mass used is less than half the xenon equivalent mass. More than 400 kg of propellant could be saved in a four thruster configuration due to the potential propellant efficiency of magnesium.

Experimental data in the high power range is limited as shown in Fig. 28 with data only available for iodine. In this case, iodine efficiency is high yet it does not outperform xenon suggesting potential limitations with iodine dissociation. Given the cost, outstanding performance and minimal heating requirements in this power class coupled with significant volume savings, iodine can be considered the primary alternative to xenon with a proven performance.

In summary, there is a consistent lack of data on alternative propellants in the high power range. In spite of this, the theoretical study suggests that iodine, bismuth zinc and magnesium would be good propellant alternatives to xenon. The advantages in terms of propellant mass, volume and propellant cost are significant over xenon in a mission scenario where heater power expenditure is minimal compared to the thruster power.

9. Conclusion

In this study, propellant alternatives to xenon have been identified and explored through their physical properties, thruster compatibility and potential performance in a Hall thruster. An experimental Hall thruster performance database was used to support the findings of the theoretical study.

The most power efficient alternative propellant identified in the low power range (≤1 kW) was iodine which can be utilized with a minimal heater power expenditure providing similar if not superior performance to xenon at a lower cost and higher density. TPA and TEA also benefit from modest heating requirements and offer promising preliminary performance.

In the mid power range (1 kW-2.5 kW), iodine, zinc, and bismuth were identified as the most promising alternatives. Bismuth was shown experimentally and theoretically to have an excellent performance in terms of thrust and anode efficiency compared to xenon. However the high heater power requirement makes it less desirable in this power bracket. Iodine was still classified as a good alternative to xenon in the medium power bracket. Zinc was identified as the most theoretically promising propellant alternative to xenon through the high density, lower propellant mass requirement, low cost and low heater power requirements coupled with the demonstrated efficient experimental performance.

The high power range (≥2.5 kW) was proposed as the perfect power level for bismuth usage. Zinc and magnesium were also shown to be capable of providing significant benefits to xenon usage in this power level. The high density, lower propellant mass requirement, low cost and low heater power requirements of zinc and magnesium make them desirable propellants in this power bracket along with bismuth. Finally, iodine was shown to maintain good performance both theoretically and experimentally making it a good alternative to xenon in the high power range.

Molecular propellants present benefits in terms of theoretically achievable performance both as high thrust alternatives (C_{60}) as well as molecular weight similarity to xenon (TPA, TEA and adamantane). Experimentally, oxygen, carbon dioxide and water demonstrate through preliminary data potential for in-situ utilization at the expense of lower anode efficiency.

Atomic gasses such as argon and krypton were compared directly to xenon and shown to exhibit a lower theoretical and experimental performance in most power brackets which was surpassed by other alternatives.

The associated reactivity of elements such as iodine, TEA, and TPA may pose significant engineering challenges at a system level integration with the spacecraft. The associated high vapor pressure of adamantane, TEA, TPA, and iodine at low temperature may increase the surface contamination rate by promotion of secondary sublimation spots on spacecraft surfaces resulting from temperature cycles.

Ground testing and development of thrusters utilizing corrosive, reactive, or toxic propellants may be slower due to the imposed safety and control standards. Through condensation and inherent lower vapor pressure, elements such as C_{60}, zinc, bismuth, and magnesium can

maintain low vacuum pressure even at high flow rates and within confined volumes. Utilizing these elements as propellants enables ground testing of very high power thrusters and thruster development in lower volume/ pumping capacity vacuum chambers.

To this date, krypton remains the most common alternative to xenon prevalent in the space industry, with a significant cost associated. This cost is lower than xenon, although much higher than the cost of the propellants analyzed in this paper.

It is clear though that there is a need to move away from the very predominate use of xenon in electric propulsion, and that there are alternatives that have been experimentally demonstrated to suit a variety of mission scenarios. There are better and more sustainable options to xenon and still more potential propellants to be explored.

Declaration of competing interest

The authors declare the following financial interests/personal relationships which may be considered as potential competing interests: Vlad-George Tirila reports financial support was provided by OHB Sweden AB.

Acknowledgment

The authors would like to thank OHB Sweden for supporting this research through Ph.D. funding.

References

[1] A. Shagayda, On scaling of Hall effect thrusters, IEEE Trans. Plasma Sci. 43 (2015) 12–28.
[2] D. Lev, R. Myers, K. Lemmer, K. Kolbeck, J., H.K. Polzin, The technological and commercial expansion of electric propulsion, Acta Astronaut. 159 (2019) 213–227.
[3] I. Levchenko, K. Bazaka, Y. Ding, Y. Raitses, S. Mazouffre, T. Henning, P.J. Klar, S. Shinohara, J. Schein, L. Garrigues, et al., Space micropropulsion systems for cubesats and small satellites: From proximate targets to furthermost frontiers, Appl. Phys. Rev. 5 (1) (2018) 011104.
[4] J. Gonzalez del Amo, European space agency (ESA) electric propulsion activities, in: 34th International Electric Propulsion Conference (IEPC), Kobe, 2015, pp. 4–10.
[5] D.Y. Oh, S. Collins, T. Drain, W. Hart, T. Imken, K. Larson, D. Marsh, D. Muthulingam, J.S. Snyder, D. Trofimov, et al., Development of the psyche mission for NASA's discovery program, in: 36th International Electric Propulsion Conference, Pasadena, CA: Jet Propulsion Laboratory, National Aeronautics and Space, 2019.
[6] J.C. McDowell, The low earth orbit satellite population and impacts of the spacex starlink constellation, Astrophys. J. Lett. 892 (2) (2020) L36.
[7] Y. Henri, The OneWeb satellite system, Handb. Small Satell.: Technol., Des., Manuf. Appl., Econ. Regul. (2020) 1–10.
[8] R. Morales-Ferre, E.S. Lohan, G. Falco, E. Falletti, GDOP-based analysis of suitability of LEO constellations for future satellite-based positioning, in: 2020 IEEE International Conference on Wireless for Space and Extreme Environments, (WiSEE), 2020, pp. 147–152.
[9] P. Abbasrezaee, M. Mirshams, S. Seyed-Zamani, Conceptual GEO telecommunication all-electric satellite design based on statistical model, in: 2019 9th International Conference on Recent Advances in Space Technologies, (RAST), 2019, pp. 503–507.
[10] P. Abbasrezaee, A. Saraaeb, System analysis and design of the geostationary earth orbit all-electric communication satellites, J. Aerosp. Technol. Manag. 13 (2021).
[11] D. Herman, T. Tofil, Overview of the development and mission application of the advanced electric propulsion system (AEPS), 2018.
[12] D. Oh, S. Collins, Development of the psyche mission for NASA's discovery program, in: 35th International Electric Propulsion Conference, (IEPC), 2017.
[13] S. Le May, S. Gehly, B. Carter, S. Flegel, Space debris collision probability analysis for proposed global broadband constellations, Acta Astronaut. 151 (2018) 445–455.
[14] D. O'Reilly, G. Herdrich, D.F. Kavanagh, Electric propulsion methods for small satellites: A review, Aerospace 8 (1) (2021) 22.
[15] P. Häussinger, R. Glatthaar, W. Rhode, H. Kick, C. Benkmann, J. Weber, H.-J. Wunschel, V. Stenke, E. Leicht, H. Stenger, Noble gases, Ullmann's Encyclopedia Ind. Chem. (2000).
[16] D. Herman, K. Unfried, Xenon acquisition strategies for high-power electric propulsion NASA missions, in: 62nd JANNAF Propulsion Meeting, Nashville, TN, 2015.
[17] E.-N. Glueckauf, G. Kitt, The krypton and xenon contents of atmospheric air, Proc. R. Soc. London Ser. A Math. Phys. Sci. 234 (1199) (1956) 557–565.
[18] A. Neice, M. Zornow, Xenon anaesthesia for all, or only a select few? Anaesthesia 71 (11) (2016) 1267–1272.
[19] N.M. Ngoc, D.T. Viet, N.H. Tien, P.M. Hiep, N. Anh, L. Anh, N. Truong, N. Anh, L. Trung, V. Dung, et al., Russia-Ukraine war and risks to global supply chains, Int. J. Mech. Eng. 7 (2022) 633–640.
[20] F.B. Insights, Xenon market size, share & COVID-19 impact analysis, by type (N3, N4.5, and N5), by application (imagining & lighting, satellite, electronics & semiconductors, medical, and others), and regional forecast, 2022–2029, 2022, (2022) Accessed on 1/09/2023, URL https://www.fortunebusinessinsights.com/xenon-market-101965.
[21] J. Szabo, M. Robin, et al., Light metal propellant Hall thrusters, in: 31st International Electric Propulsion Conference (IEPC), Vol. IEPC-2009-138, 2009.
[22] J. Szabo, M. Robin, Bismuth vapor Hall effect thruster performance and plume experiments, in: 35th International Electric Propulsion Conferenc, (IEPC), 2017.
[23] J. Makela, R. Washeleski, Development of a magnesium and zinc Hall-effect thruster, J. Propul. Power 26 (2010) 1029.
[24] M. Hopkins, L. King, Performance comparison between a magnesium-and xenon-fueled 2 kilowatt Hall thruster, J. Propul. Power (2016) 1015–1021.
[25] J. Szabo, B. Pote, Performance evaluation of an iodine-vapor Hall thruster, J. Propul. Power 28 (2012) 848–857.
[26] R. Moloney, Performance and behaviour of unconventional molecular propellants in a cylindrical Hall thruster, in: Space Propulsion Conference, 2020.
[27] T. Schönherr, K. Komurasaki, F. Romano, B. Massuti-Ballester, G. Herdrich, Analysis of atmosphere-breathing electric propulsion, IEEE Trans. Plasma Sci. 43 (1) (2014) 287–294.
[28] J. Linnell, A. Gallimore, Efficiency analysis of a Hall thruster operating with krypton and xenon, J. Propul. Power 22 (2006) 1402–1418.
[29] M.R. Nakles, W.A. Hargus Jr., J.J. Delgado, R.L. Corey, A performance comparison of xenon and krypton propellant on an SPT-100 Hall thruster, in: 32nd International Electric Propulsion Conference (IEPC), Vol. IEPC-2011-003, Wiesbaden, Germany, 2011.
[30] J. Kurzyna, M. Jakubczak, Performance tests of IPPLM's krypton Hall thruster, Laser Part. Beams 36 (2018) 105.
[31] G. Xia, H. Li, Performance optimization of a krypton Hall thruster with a rotating propellant supply, Acta Astronaut. (2020) (2020).
[32] Z. Ning, G. Xia, Research on beam-focusing characteristics of krypton Hall thruster, Plasma Phys. Rep. 45 (2019) 537–550.
[33] J. Lim, I. Levchenko, Plasma parameters and discharge characteristics of lab-based krypton-propelled miniaturized Hall thruster, Plasma Sources. Sci. Technol. 28 (2019) 064003.
[34] D.T. Jacobson, D.M. Manzella, 50 KW class krypton Hall thruster performance, in: 39th Joint Propulsion Conference and Exhibit, 2003.
[35] T. Nagayoshi, T. Izuki, H. Tahara, T. Ikeda, Y. Takao, Propulsion performance of Hall thrusters for solar system space navigation -materials on planets and satellites: Use of carbon dioxide, methane, ammonia, hydrogen, helium, air, ice and water as propellants, in: 37th International Electric Propulsion Conference (IEPC), Vol. IEPC-2022-282, Boston, USA, 2022.
[36] R.R. Hofer, P.Y. Peterson, D.T. Jacobson, D.M. Manzella, Factors affecting the efficiency of krypton Hall thrusters, in: 46th Meeting of the APS Division of Plasma Physics, 2004.
[37] D.M. Goebel, I. Katz, Fundamentals of Electric Propulsion: Ion and Hall Thrusters, John Wiley & Sons, 2008.
[38] L.L. Su, B. Jorns, Performance at high current densities of a magnetically-shielded Hall thruster, in: AIAA Propulsion and Energy 2021 Forum, 2021, p. 3405.
[39] G. Cann, G. Marlotte, Hall current plasma accelerator, AIAA J. 2 (1964) 1234–1241.
[40] G. Krülle, E. Zeyfang, Preliminary conclusions of continuous applied field electromagnetic thruster research at DFVLR, in: 11th International Electric Propulsion Conference, (IEPC), 1975.
[41] R. Koehne, F. Lindner, Further investigations on low-density Hall accelerators, AIAA J. 8 (1970) 873–879.
[42] V. Zhurin, A. Porotnikov, Electric propulsion research and development in the USSR, in: 12th International Electric Propulsion Conference, (IEPC), 1976.
[43] V. Kim, G. Popov, Investigation of SPT performance and particularities of it's operation with kr and Kr/Xe mixtures, in: 27th International Electric Propulsion Conference, (IEPC), Pasadena, CA, 2001, pp. 01–065.
[44] C. Ducci, T. Andreussi, A. Arkhipov, A. Passaro, M. Andrenucci, A. Bulit, C. Edwards, Investigation of a 5 kw class Hall-effect thruster operating with different xenon-krypton mixtures, in: 34th International Electric Propulsion Conference, (IEPC), 2015.
[45] B. Arkhipov, A. Koryakin, V. Murashko, A. Nesterenko, I. Khoromsky, V. Kim, V. Kozlov, G. Popov, A. Skrylnikov, The results of testing and effectiveness of the kr-xe mixture application in SPT, in: 27th International Electric Propulsion Conference, (IEPC), 2001.
[46] J. Yamasaki, S. Yokota, K. Shimamura, Performance enhancement of an argon-based propellant in a Hall thruster, Vacuum 167 (2019) 520–523.

[47] T. Andreussi, E. Ferrato, Development status and way forward of SITAEL's air-breathing electric propulsion engine, AIAA Propul. Energy, (2019) (2019).
[48] V. Hruby, K. Hohman, J. Szabo, Air breathing Hall effect thruster design studies and experiments, in: 37th International Electric Propulsion Conference, (IEPC), Boston, MA, 2022.
[49] A. Kieckhafer, L.B. King, Energetics of propellant options for high-power Hall thrusters, J. Propul. Power 23 (1) (2007) 21–26.
[50] O. Tverdokhlebov, A. Semenkin, Iodine propellant for electric propulsion-to be or not to be, in: 37th Joint Propulsion Conference and Exhibit, 2001.
[51] D. Rafalskyi, J.M. Martínez, L. Habl, E. Zorzoli Rossi, P. Proynov, A. Boré, T. Baret, A. Poyet, T. Lafleur, S. Dudin, et al., In-orbit demonstration of an iodine electric propulsion system, Nature 599 (7885) (2021) 411–415.
[52] D. Massey, A. Kieckhafer, Development of a vaporizing liquid bismuth anode for Hall thrusters, in: 40th AIAA/ASME/SAE/ASEE Joint Propulsion Conference and Exhibit, 2004.
[53] C. Marrese-Reading, A. Sengupta, VHITAL program to demonstrate the performance and lifetime of a bismuth-fueled very high isp Hall thruster, in: 41st Joint Prop. Conf, Vol. AIAA-2005-4564, Tucson, Arizona, 2005.
[54] M. Hopkins, J. Makela, Mass flow control in a magnesium Hall-effect thruster, in: 46th AIAA/ASME/SAE/ASEE Joint Propulsion Conference & Exhibit, 2010.
[55] E. Pinsley, C. Brown, Hall-current accelerator utilizing surface contact ionization, J. Spacecr. Rockets 1 (1964) 525–531.
[56] C. Brown, E. Pinsley, Further experimental investigations of a cesium Hall-current accelerator, AIAA J. 3 (1965) 853–859.
[57] E. Pinsley, Characteristics of a surface contact Hall current accelerator, IEEE Trans. Nucl. Sci. 11 (1964) 58–65.
[58] G.W. Thomson, The antoine equation for vapor-pressure data., Chem. Rev. 38 (1) (1946) 1–39.
[59] D. Koutsoyiannis, Clausius–Clapeyron equation and saturation vapour pressure: simple theory reconciled with practice, Eur. J. Phys. 33 (2) (2012) 295.
[60] National Institude of Standards and Technology, NIST Chemistry WebBook, "Iodine".
[61] C. Alcock, V. Itkin, Vapour pressure equations for the metallic elements: 298–2500K, Can. Metall. Q. 23 (1984) 309–313.
[62] M. Tsay, J. Frongillo, K. Hohman, Iodine-fueled mini RF ion thruster for CubeSat applications, in: 34th International Electric Propulsion Conference (IEPC), Kobe, Japan, 2015.
[63] J.M. Martinez, D. Rafalskyi, Development of iodine propellant and flow control units suitable for multiple propulsion systems, in: Space Propulsion Conference, 2020.
[64] K. Polzin, J. Seixal, Et al. The iodine satellite (isat) propellant feed system-design and demonstration, in: 35th International Electric Propulsion Conference (IEPC), Vol. 1, (IEPC-2017-11) Atlanta, Georgia, 2017.
[65] V.-G. Tirila, A. Hallock, A. Demairé, C.N. Ryan, Zinc propellant storage and delivery system for Hall thrusters, in: AIAA Propulsion and Energy 2021 Forum, 2021, p. 3407.
[66] V. Tirila, C. Ryan, A. Demairé, A. Hallock, Performance investigation of zinc propellant in sub kw class Hall thrusters, in: 37th International Electric Propulsion Conference, (IEPC), Boston, MA, 2022.
[67] M.A. Hopkins, Evaluation of Magnesium as a Hall Thruster Propellant, Michigan Technological University, 2015.
[68] S. Tverdokhlebov, A. Semenkin, Bismuth propellant option for very high power TAL thruster, AIAA J. 348 (2002).
[69] K.B. Panfilovich, V.V. Sagadeev, I.L. Golubeva, Thermal radiation of binary alloys of tin, lead, and bismuth, High Temp. 42 (5) (2004) 720–726.
[70] J. Safarian, T. Engh, Vacuum evaporation of pure metals, Metall. Mater. Trans. A 44 (2013) 747–753.
[71] F. Paganucci, D. Pedrini, L. Bernazzani, A. Ceccarini, M.M. Saravia, Development of an iodine propellant feeding system for electric propulsion, in: Space Propulsion, 2016.
[72] C.F. Colebrook, T. Blench, H. Chatley, E. Essex, J. Finniecome, G. Lacey, J. Williamson, G. Macdonald, Correspondence. turbulent flow in pipes, with particular reference to the transition region between the smooth and rough pipe laws.(includes plates), J. Inst. Civ. Eng. 12 (8) (1939) 393–422.
[73] B. McKeon, C. Swanson, M. Zagarola, R. Donnelly, A.J. SMITS, Friction factors for smooth pipe flow, J. Fluid Mech. 511 (2004) 41–44.
[74] A. Avci, I. Karagoz, A new explicit friction factor formula for laminar, transition and turbulent flows in smooth and rough pipes, Eur. J. Mech. B Fluids 78 (2019) 182–187.
[75] B.E. Poling, J.M. Prausnitz, J.P. O'connell, et al., The Properties of Gases and Liquids, Vol. 5, Mcgraw-hill New York, 2001.
[76] R.A. Svehla, Estimated Viscosities and Thermal Conductivities of Gases At High Temperatures, Vol. 132, National Aeronautics and Space Administration, 1963.
[77] J.M. Martínez, D. Rafalskyi, E.Z. Rossi, A. Aanesland, Development, qualification and first flight data of the iodine based cold gas thruster for CubeSats, in: 5th IAA Conference on University Satellite Missions and CubeSat Workshop, 2020.
[78] M. Tsay, J. Model, C. Barcroft, J. Frongillo, J. Zwahlen, C. Feng, Integrated testing of iodine bit-3 rf ion propulsion system for 6u cubesat applications, in: 35th International Electric Propulsion Conference (IEPC), Atlanta, USA, 2017.
[79] H.R. Kaufman, Technology of closed-drift thrusters, AIAA J. 23 (1) (1985) 78–87.
[80] G. Eschard, A. Pelissier, J. Paulin, J. Bonnal, Experimental studies of a linear strip cesium contact ion thruster, J. Spacecr. Rockets 13 (4) (1976) 193–197.
[81] T.D. Masek, Experimental Studies with a Mercury Bombardment Thrustor System, Tech. rep., 1968.
[82] T. Masek, Plasma properties and performance of mercury ion thrusters, AiAA Journal 9 (2) (1971) 205–212.
[83] W. Kerslake, L. Ignaczak, Development and flight history of SERT II spacecraft, AIAA 92 (1992) 3516.
[84] R.A. Bernhoft, Mercury toxicity and treatment: a review of the literature, J. environmental and public health 2012 (2012).
[85] W.C. Butterman, W.E. Brooks, R.G. Reese Jr., Mineral commodity profiles: cesium, US Geol. Surv. Open-File Rep. 2004 (2005) 1432.
[86] J. Antill, K. Peakall, E. Smart, Corrosion of stainless steel in the presence of caesium, J. Nucl. Mater. 56 (1) (1975) 47–60.
[87] D. Hall, B. Newnam, Electrostatic rocket exhaust effects on solar-electric spacecraft subsystems, J. Spacecr. Rockets 7 (1970) 305–312.
[88] A. Kieckhafer, D. Massey, Performance and active thermal control of a 2-kW Hall thruster with segmented electrodes, J. Propul. Power 23 (2007) 821–827.
[89] V. Gnedenko, V. Petrosov, Prospects for using metals as propellant in stationary plasma engines of Hall-type, in: 24th International Electric Propulsion Conference, (IEPC), Moscow, Russia, 1996.
[90] M. Crofton, K. Diamant, A preliminary study of contamination effects in a bismuth Hall thruster environment, in: 41st AIAA/ASME/SAE/ASEE Joint Propulsion Conference & Exhibit, 2005.
[91] J. Pollard, K. Diamant, Hall thruster plume shield wake structure, in: 39th AIAA/ASME/SAE/ASEE Joint Propulsion Conference and Exhibit, 2003.
[92] J. Szabo, M. Robin, Et al. High density Hall thruster propellant investigations, in: 48th AIAA/ASME/SAE/ASEE Joint Propulsion Conference & Exhibit, Vol. AIAA 2012-3853, Atlanta Georgia, 2012.
[93] M. Hopkins, L. King, Magnesium Hall thruster with active thermal mass flow control, J. Propul. Power 30 (2014) 637–644.
[94] F. Czerwinski, Controlling the ignition and flammability of magnesium for aerospace applications, Corros. Sci. 86 (2014) 1–16.
[95] T. Miller, J. Herr, Green rocket propulsion by reaction of Al and Mg powders and water, in: 40th AIAA/ASME/SAE/ASEE Joint Propulsion Conference and Exhibit, 2004.
[96] J. Linnell, T. Miller, A preliminary design of a magnesium fueled martian ramjet engine, in: 38th AIAA/ASME/SAE/ASEE Joint Propulsion Conference & Exhibit, 2002.
[97] A. Janes, D. Carson, A. Accorsi, J. Chaineaux, B. Tribouilloy, D. Morainvillers, Correlation between self-ignition of a dust layer on a hot surface and in baskets in an oven, J. Hazard. Mater. 159 (2–3) (2008) 528–535.
[98] U.G. Survey, Mineral commodity summaries 2022, U.S. Geol. Surv. (2022).
[99] M. Hopkins, L. King, Condensable propellant Hall thruster for metallic thin film deposition, in: 52nd AIAA/SAE/ASEE Joint Propulsion Conference, 2016.
[100] R. Dressler, Y.-H. Chiu, Propellant alternatives for ion and Hall effect thrusters, in: 38th Aerospace Sciences Meeting and Exhibit, 2000.
[101] J. Szabo, M. Robin, Et al. Iodine propellant space propulsion, in: 33rd International Electric Propulsion Conference (IEPC), Vol. IEPC-2013-311, Wasington DC, USA, 2013.
[102] G. Benavides, H. Kamhawi, Et al. Iodine Hall-effect electric propulsion system research, development, and system durability demonstration, in: Joint Prop. Conf, Vol. AIAA–2018–4422, Cincinnati, Ohio, 2018.
[103] J. Szabo, M. Robin, Iodine plasma propulsion test results at 1–10 kW, IEEE Trans. Plasma Sci. 43 (2014) 141–148.
[104] P. Grondein, T. Lafleur, Global model of an iodine gridded plasma thruster, Phys. Plasmas 23 (2016) 033514.
[105] D. Martinez, A. Aanesland, Development and testing of the NPT30-I2 iodine ion thruster, in: 36th International Electric Propulsion Conference, (IEPC), 2019.
[106] M. Vaupel, N. Gerrit Kottke, Et al. Advanced cusp field thruster with a 3D-printed discharge channel - performance with iodine and xenon, in: 36th International Electric Propulsion Conference (IEPC), Vol. IEPC-2019-a-621, Vienna, Austria, 2019.
[107] M. Manente, F. Trezzolani, Know-how acquired on iodine propellant, in: 36th International Electric Propulsion Conference (IEPC), Vol. IEPC-2019-419, Vienna, Austria, 2019.
[108] K. Polzin, D. Bradley, Iodine beam dump design and fabrication, NASA Tech. Memo. (TM) (2017) (2017).
[109] W. Gartner, D. Zschatzsch, Characterization of the operation of RITs with iodine, in: 35th International Electric Propulsion Conference (IEPC), Vol. IEPC-2017-368, Atlanta, Georgia, 2017.
[110] R. Rejoub, B. Lindsay, Determination of the absolute partial and total cross sections for electron-impact ionization of the rare gases, Phys. Rev. A 65 (2002) 042713.
[111] P. Bartlett, A. Stelbovics, Electron-impact ionization cross sections for elements Z=1 to Z=54, At. Data Nucl. Data Tables 86 (2004) 235–265.
[112] M. Gryziński, Two-particle collisions. II. Coulomb collisions in the laboratory system of coordinates, Phys. Rev. 138 (2A) (1965) A322.

[113] H. Bittrich, M. Kulanek, G. Duering, Zur thermodynamik des systems Diäthylamin-Triäthylamin, Z. Phys. Chem. 219 (1) (1962) 387–401.
[114] C. Gobble, J. Vikman, J.S. Chickos, Evaluation of the vaporization enthalpies and liquid vapor pressures of (R)-Deprenyl,(S)-Benzphetamine, alverine, and a series of aliphatic tertiary amines by correlation gas chromatography at T/K=298.15, J. Chem. Eng. Data 59 (8) (2014) 2551–2562.
[115] A.L. Buck, New equations for computing vapor pressure and enhancement factor, J. Appl. Meteorol. Climatol. 20 (12) (1981) 1527–1532.
[116] A.B. Bazyleva, A.V. Blokhin, G.J. Kabo, M.B. Charapennikau, V.N. Emel'yanenko, S.P. Verevkin, V. Diky, Thermodynamic properties of adamantane revisited, J. Phys. Chem. B 115 (33) (2011) 10064–10072.
[117] E. Schönherr, K. Matsumoto, M. Freiberg, On the evaporation of C60 in vacuum and inert gases at temperatures between 830 k and 1050 k, Fullerene Sci. Technol. 7 (3) (1999) 455–466.
[118] V. Piacente, G. Gigli, P. Scardala, A. Giustini, D. Ferro, Vapor pressure of C60 buckminsterfullerene, J. Phys. Chem. 99 (38) (1995) 14052–14057.
[119] K. Patrick Dietz, K. Holste, P. Waldemar Gartner, P.J. Klar, P.S. R, Status report of diamondoids as alternative propellants for ion-thrusters, in: 35th International Electric Propulsion Conference (IEPC), Vol. IEPC-2017-198, 2017.
[120] J. Kolosnjaj, H. Szwarc, F. Moussa, Toxicity studies of fullerenes and derivatives, Bio-Applications of nanoparticles (2007) 168–180.
[121] K. Lenzke, L. Landt, M. Hoener, H. Thomas, J. Dahl, S. Liu, R. Carlson, T. Möller, C. Bostedt, Experimental determination of the ionization potentials of the first five members of the nanodiamond series, J. Chem. Phys. 127 (8) (2007) 084320.
[122] P. Dietz, W. Gärtner, Q. Koch, P.E. Köhler, Y. Teng, P.R. Schreiner, K. Holste, P.J. Klar, Molecular propellants for ion thrusters, Plasma Sources. Sci. Technol. 28 (8) (2019) 084001.
[123] M.A. Bretti, Progress and developments of ultra-compact 10 watt class adamantane fueled Hall thrusters for picosatellites, in: 37th International Electric Propulsion Conference (IEPC), Vol. IEPC-2022-349, Boston, USA, 2022.
[124] S. Leifer, D. Rapp, Electrostatic propulsion using C60 molecules, J. Propul. Power 8 (1992) 1297–1300.
[125] J. Anderson, D. Fitzgerald, Experimental investigation of fullerene propellant for ion propulsion, in: 23rd International Electric Propulsion Conference (IEPC), Vol. IEPC-93-033, October, Seattle, WA, 1993.
[126] C. Scharlemann, Theoretical and experimental investigation of C60-propellant for ion propulsion, Acta Astronaut. 51 (2002) 865–872.
[127] S. Matt, B. Dünser, M. Lezius, H. Deutsch, K. Becker, A. Stamatovic, P. Scheier, T. Märk, Absolute partial and total cross-section functions for the electron impact ionization of C60 and C70, J. Chem. Phys. 105 (5) (1996) 1880–1896.
[128] N. Kumar, S. Pal, Evaluation of direct ionization cross sections for C60 by electron interaction, J. Phys.: Conf. Ser. 163 (1) (2009) 012029.
[129] J. Szabo, J. Frongillo, S. Gray, Z. Taillefer, Fullerene propellant Hall thruster experiment, in: 37th International Electric Propulsion Conference, (IEPC), Boston, USA, 2022.
[130] M. Abbi, M. Tejeda, A. Knoll, Investigation into the wall interactions of a Hall effect thruster using water vapor as a propellant, in: 37th International Electric Propulsion Conference, (IEPC), Boston, MA, 2022.
[131] A. Schwertheim, A. Knoll, Experimental investigation of a water electrolysis Hall effect thruster, Acta Astronaut. 193 (2022) 607–618.
[132] K. Shirasu, H. Kuwabara, Far-field plume diagnostics of low-power water Hall thruster, in: 37th International Electric Propulsion Conference, (IEPC), Boston, MA, 2022.
[133] A. Schwertheim, C. Muir, A. Knoll, Experimentally demonstrating the feasibility of water as a multimode electric-chemical propellant, in: 37th International Electric Propulsion Conference, (IEPC), Boston, MA, 2022.
[134] C. Champion, J. Hanssen, P.-A. Hervieux, Electron impact ionization of water molecule, Chem. Phys. - Chem. Phys. 117 (2002).
[135] M. Bolorizadeh, M.E. Rudd, Angular and energy dependence of cross sections for ejection of electrons from water vapor. I. 50–2000-eV electron impact, Phys. Rev. A 33 (2) (1986) 882.
[136] C. Muir, A. Knoll, Catalytic combustion of hydrogen and oxygen, Gen. Issue (2019) 2.
[137] A. Schwertheim, A. Knoll, The water electrolysis Hall effect thruster (wet-het): Paving the way to dual mode chemical-electric water propulsion, in: 36th International Electric Propulsion Conference, (IEPC), 2019, p. 259.
[138] E.R. Azevedo, K. Jones-Tett, H. Larsen, S. Reeve, E. Longhi, J.M.M. Tejeda, R. Moloney, A. Schwertheim, A. Knoll, Sizing and preliminary design of a 2-kW water propelled Hall effect thruster, in: 37th International Electric Propulsion Conference, (IEPC), Boston, MA, 2022.
[139] E. Ferrato, V. Giannetti, A. Piragino, M. Andrenucci, T. Andreussi, C.A. Paissoni, Development roadmap of sitael's RAM-EP system, in: 36th International Electric Propulsion Conference (IEPC), Vol. IEPC-2019-886, 2019.
[140] F. Marchioni, M.A. Cappelli, Extended channel Hall thruster for air-breathing electric propulsion, J. Appl. Phys. 130 (5) (2021) 053306.
[141] H. Straub, P. Renault, B. Lindsay, K. Smith, R. Stebbings, Absolute partial cross sections for electron-impact ionization of H 2, N 2, and O 2 from threshold to 1000 eV, Phys. Rev. A 54 (3) (1996) 2146.
[142] D. Margreiter, H. Deutsch, M. Schmidt, T. Märk, Electron impact ionization cross sections of molecules: Part II. Theoretical determination of total (counting) ionization cross sections of molecules: A new approach, Int. J. Mass Spectrom. Ion Processes 100 (1990) 157–176.
[143] G. Cifali, T. Misuri, P. Rossetti, M. Andrenucci, D. Valentian, D. Feili, Preliminary characterization test of HET and RIT with nitrogen and oxygen, in: 47th AIAA/ASME/SAE/ASEE Joint Propulsion Conference & Exhibit, 2011, p. 6073.
[144] T. Andreussi, G. Cifali, Development and experimental validation of a Hall effect thruster RAM-EP concept, in: 35th International Electric Propulsion Conference, (IEPC), 2017.
[145] K. Hohman, V. Hruby, et al., Atmosphereic breathing electric thruster for planetary exploration, in: NIAC Spring Symposium, 2012.
[146] A. Gurciullo, A. Fabris, Ion plume investigation of a Hall effect thruster operating with xe/N2 and xe/air mixtures, J. Phys. D: Appl. Phys. 52 (2019) 464003.
[147] Z. Taillefer, J. Blandino, Characterization of the near-plume region of a laboratory bao hollow cathode operating on xenon and iodine propellants, in: 35th International Electric Propulsion Conference (IEPC), Vol. IEPC-2017-465, 2017.
[148] D. Goebel, G. Becatto, High current lanthanum hexaboride hollow cathode for 20-200 kw Hall thrusters, in: 35th International Electric Propulsion Conference, (IEPC), 2017.
[149] J. Makela, D. Massey, Bismuth hollow cathode for Hall thrusters, J. Propul. Power 24 (2008) 142.
[150] S. Gabriel, A. Daykin-Iliopoulos, Hollow cathode operation with different gases, in: 35th International Electric Propulsion Conference, (IEPC), 2017.
[151] D. Goebel, G. Becatto, Hollow cathode for a very high isp interstellar precursor ion thruster, in: 36th International Electric Propulsion Conference (IEPC), Vol. IEPC-2019-369, Vienna, Austria, 2019.
[152] J. Brophy, J. Grandidier, Propulsion architecture for deep-space missions with characteristic velocities of order 100 km/s, in: 36th International Electric Propulsion Conference (IEPC), Vol. IEPC-2019-361, Vienna, Austria, 2019.
[153] D. Lev, I. Mikellides, Recent progress in research and development of hollow cathodes for electric propulsion, Rev. Modern Plasma Phys. 3, 6 (2019).
[154] S. Thompson, C. Farnell, Evaluation of iodine compatible cathode configurations, in: 36th International Electric Propulsion Conference (IEPC), Vol. IEPC-2019-768, 2019.
[155] L. Rand, J. Williams, A calcium aluminate electride hollow cathode, IEEE Trans. Plasma Sci. 43 (2014) 190–194.
[156] K. Polzin, S. Peeples, Propulsion system development for the iodine satellite (iSAT), in: 34th International Electric Propulsion Conference, (IEPC), Kobe, Japan, 2015, –2015 09.
[157] T. Gancarz, W. Gasior, H. Henein, Physicochemical properties of Sb, Sn, Zn, and Sb–Sn system, Int. J. Thermophys. 34 (2) (2013) 250–266.
[158] P. McGonigal, A. Kirshenbaum, A. Grosse, The liquid temperature range, density, and critical constants of magnesium1, J. Phys. Chem. 66 (4) (1962) 737–740.
[159] M.J. Assael, I.J. Armyra, J. Brillo, S.V. Stankus, J. Wu, W.A. Wakeham, Reference data for the density and viscosity of liquid cadmium, cobalt, gallium, indium, mercury, silicon, thallium, and zinc, J. Phys. Chem. Ref. Data 41 (3) (2012) 033101.
[160] J. Cahill, A. Kirshenbaum, The density of liquid bismuth from its melting point to its normal boiling point and an estimate of its critical constants, J. Inorg. Nucl. Chem. 25 (5) (1963) 501–506.
[161] K. Dannenmayer, S. Mazouffre, Elementary scaling laws for the design of low and high power Hall effect thrusters, in: Progress in Propulsion Physics, EDP Sciences, 2009, pp. 601–616.
[162] G. Racca, A. Marini, L. Stagnaro, J. Van Dooren, L. Di Napoli, B. Foing, R. Lumb, J. Volp, J. Brinkmann, R. Grünagel, et al., SMART-1 mission description and development status, Planet. Space Sci. 50 (14–15) (2002) 1323–1337.
[163] D. Estublier, G. Saccoccia, J. Gonzales Del Amo, Electric propulsion on SMART-1-A technology milestone, ESA Bull. 129 (2007) 40–46.
[164] J.S. Snyder, V.H. Chaplin, D.M. Goebel, R.R. Hofer, A. Lopez Ortega, I.G. Mikellides, T. Kerl, G. Lenguito, F. Aghazadeh, I. Johnson, Electric propulsion for the psyche mission: Development activities and status, in: AIAA Propulsion and Energy 2020 Forum, 2020, p. 3607.
[165] D. Manzella, Performance Evaluation of the SPT-140, Vol. 206301, National Aeronautics and Space Administration, Lewis Research Center, 1997.
[166] J.S. Snyder, D.M. Goebel, V. Chaplin, A. Lopez Ortega, I.G. Mikellides, F. Aghazadeh, I. Johnson, T. Kerl, G. Lenguito, Electric propulsion for the psyche mission, in: 36th International Electric Propulsion Conference, (IEPC), JPL Open Repository, 2019.